US EPA ARCHIVE DOCUMENT

US EPA ARCHIVE DOCUMENT

INCORPORATION OF HETEROGENEITY INTO MONTE-CARLO FATE AND TRANSPORT SIMULATIONS

Work Assignment Manager and Technical Directions:
Dr. Zubair A. Saleem
U.S. Environmental Protection Agency
Office of Solid Waste
Washington, DC 20460

Prepared by:
HydroGeoLogic, Inc
1155 Herndon Parkway, Suite 900
Herndon, VA 20170
Under Contract No. 68-W7-0035

U.S. Environmental Protection Agency
Office of Solid Waste
Washington, DC 20460

July 1999

draft

US EPA ARCHIVE DOCUMENT

TABLE OF CONTENTS

Page

draft

US EPA ARCHIVE DOCUMENT

LIST OF FIGURES

LIST OF TABLES

Page

US EPA ARCHIVE DOCUMENT

draft

US EPA ARCHIVE DOCUMENT

Acknowledgments

A number of individuals have been involved with this development. Dr. Zubair A. Saleem of the U.S.EPA, Office of Solid Waste, provided overall technical coordination and review throughout this work. Dr. Varut Guvanasen of HydroGeoLogic, Inc. developed the procedure to determine the distributions of correction factors. Dr. Jeongkon Kim of HydroGeoLogic, Inc. was responsible for the implementation of the algorithm, and the development of the distribution functions. The model runs and data compilation were performed by Mr. Sean Stanford of HydroGeoLogic, Inc. The Fourier Spectral technique software used in the generation of random fields was provided by Dr. Edward Sudicky of University of Waterloo. The information on the variance of hydraulic conductivity was provided by Dr. Steve Schmelling of the National Risk Management Research Laboratory, and Drs. Sang B. Lee and Jin-Song Chen of Dynamac Corporation. This report was prepared primarily by Drs. V. Guvanasen and J. Kim.

DISCLAIMER

The work presented in this document has been funded by the United States Environmental Protection Agency. Mention of trade names or commercial products does not constitute endorsement or recommendation for use by the Agency.

draft

1.0 INTRODUCTION

The EPA's Composite Model for leachate migration with Transformation Products (EPACMTP) code, is used by EPA (the Office of Solid Waste) to simulate the fate and transport of contaminants leaching from a land-based waste management unit through the underlying unsaturated and saturated zones. EPACMTP replaces EPACML (U.S. EPA, 1990) as the best available tool to predict potential exposure at a downstream receptor well. EPACMTP offers improvements to EPACML by considering: 1) the formation and transport of transformation products; 2) the impact of groundwater mounding on groundwater velocity; 3) finite source as well as continuous source scenarios; and 4) metals transport.

Fate and transport processes simulated by the model include: advection, hydrodynamic dispersion, linear or nonlinear sorption, and chain-decay reactions. In cases where degradation of a waste constituent yields daughter products that are of concern, EPACMTP accounts for the formation and transport of up to six different daughter products. The composite model consists of a one-dimensional module that simulates infiltration and dissolved constituent transport through the unsaturated zone, which is coupled with a three-dimensional groundwater flow and a three-dimensional transport sub-module. The saturated zone groundwater flow sub-module accounts for the effects of leakage from the land disposal unit and regional recharge on the magnitude and direction of groundwater flow. The saturated zone transport sub-module accounts for three-dimensional advection and dispersion, chain decay reactions with up to seven different chemical species (i.e., parent with up to six daughter products), and linear or nonolinear equilibrium sorption.

However, EPACMTP is based on an assumption that the material properties in the vadose and saturated zones are homogeneous. In reality, aquifer material properties are spatially variable. In this report an approach to incorporate heterogeneity into EPACMTP is discussed. The approach has been incorporated into the HWIR99 aquifer module (U.S.EPA, 1998).

US EPA ARCHIVE DOCUMENT

US EPA ARCHIVE DOCUMENT

2.0 SIMULATION OF HETEROGENEITY

2.1 OVERVIEW

The effects of physical heterogeneity of the porous medium on the distribution of chemical concentration in a spatially heterogeneous aquifer were assessed. The assessment was conducted by comparing the distributions of chemical concentrations predicted by a fate and transport model based on a heterogeneous porous medium to those predicted by the same model based on an approximately equivalent homogeneous porous medium. The following assumptions were adopted:

- The flow is steady-state;
- The transport of chemical is steady-state;
- The chemical is non-reactive and conservative; and
- The dispersivities are scale-independent.

The first assumption is consistent with the flow regime currently used in EPACMTP (U.S.EPA, 1996, 1997 a-c) and the corresponding segregated modules (U.S. EPA, 1999). The second assumption was adopted to isolate the effects due to the heterogeneity of sorption. Although it is recognized that heterogeneity of sorption characteristics also contributes to the distribution of contaminant concentrations, it is beyond the scope of current investigation. The third assumption was adopted to isolate the effects of reaction and degradation. The fourth assumption was adopted to isolate the effects of scale dependency. The dispersivities that are not scale-dependent correspond to local dispersivities. The scale dependency of macro-scale dispersivity is related to the heterogeneity of flow and transport parameters (Gelhar, 1993).

By excluding the transient flow and transport regimes and assuming that there is no scale dependency in dispersivities, the remaining key parameters of interest are hydraulic conductivity (K) and effective porosity (ϕ). In this study, two cases of correlation were investigated: correlated and uncorrelated. For the correlated case, spatially variable effective porosity random fields were generated using the Fourier spectral technique of Robin et al. (1993). For the uncorrelated case, the porosity and hydraulic conductivity random fields were individually generated, using also the Fourier spectral technique.

Assuming a perfect correlation between hydraulic conductivity and porosity, the hydraulic conductivity fields were calculated as a function of porosity and the mean grain size diameter using the Kozeny-Carmen relation (Bear, 1979), shown below:

$$K = \frac{\rho g}{\mu}\left(\frac{\varphi^3}{(1-\varphi)^2}\,\frac{d^2}{180}\right) \qquad (2.1)$$

where:

ρ	=	Fluid density
μ	=	Dynamic viscosity of fluid
g	=	the gravitational acceleration
d	=	mean grain size diameter.

In EPACMTP, hydraulic conductivity is correlated with effective porosity using the following empirical correlation of Davis (1969):

$$d = \frac{1}{100} \exp\left[\frac{0.0261 - \varphi}{0.0385}\right] \qquad (2.2)$$

where:

d	=	the mean particle diameter (m).

In the literature, available published information suggests that hydraulic conductivity is likely to be log-normally distributed in space. In this study, it was assumed that hydraulic conductivity is log-normally distributed. In subsurface hydrology, flow parameters such as hydraulic conductivity and transmissivity are often found to be log-normally distributed (Gelhar, 1993). Because of the correlation in Equation (2.1) and the assumed distribution of log-normality of the hydraulic conductivity, the effective porosity was also assumed to be log-normally distributed.

In this study, two distributions were used to generate the hydraulic conductivity and effective porosity random fields. The two distributions are presented in Tables 2.1, and 2.2. The two distributions were intended to cover the range of site-specific spatial variability reported in the literature.

A numerical code was used to simulate the flow and transport processes. The code selected for the simulation was MODFLOW-SURFACT, a fully integrated groundwater flow and solute transport three-dimensional finite-difference code (HydroGeoLogic, 1996) which is based on the U.S.G.S. MODFLOW code (McDonald and Harbaugh, 1988).

A definition sketch of the simulation domain is presented in Figure 2.1. The flow and transport domain is two-dimensional with an infinite source (constant concentration) located close to the upgradient end of the domain. The domain dimensions are 2,400 m and 2,000 m for the length and width, respectively. Parameters used in the simulations are listed in Table 2.1. Boundary and initial conditions are described below.

US EPA ARCHIVE DOCUMENT

US EPA ARCHIVE DOCUMENT

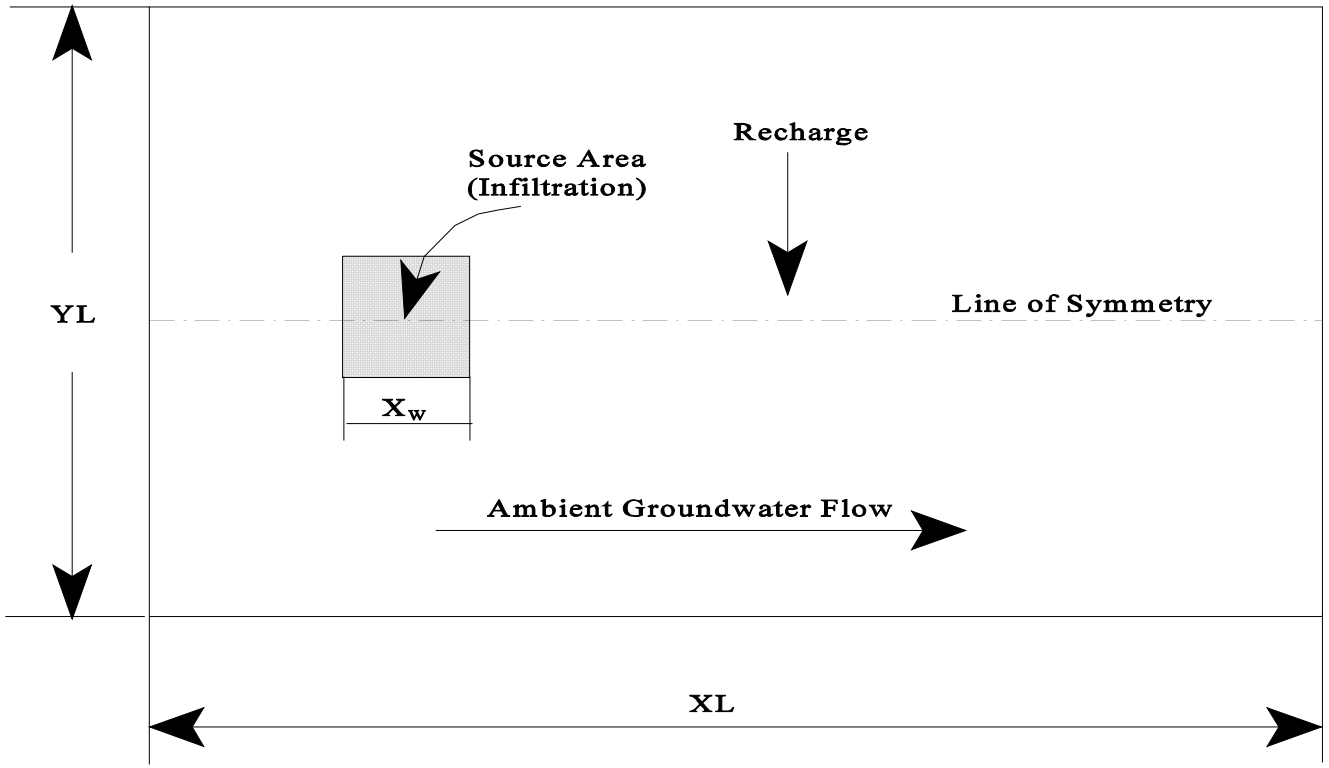

Figure 2.1 Definition Sketch of the Simulation Domain.

Table 2.1 Parameters Used in the Simulations

Parameter	Value
Layer thickness	10 m
Regional hydraulic gradient	0.006
Source infiltration rate	0.1307 m/year
Recharge rate	0.1307 m/year
Source area	19,000 m^2 (140 m x 140 m)
Longitudinal dispersivity	10, 50 , 100 m
Transverse dispersivity	0.1 x longitudinal dispersivity
Source concentration	10^6 mg/L
Grid spacing (both x and y directions)	10 m

Boundary Conditions

Hydraulic heads at the upgradient and downgradient ends were prescribed such that the regional hydraulic gradient in the x direction was 0.006. No-flow conditions were imposed along all remaining boundaries. Zero local dispersive flux normal to domain boundary was applied to all the domain boundaries.

Initial Condition

It was assumed that the aquifer had no contaminant concentration at the beginning of each simulation.

2.2 SIMULATION PROCEDURE

To study the effects of the degree of heterogeneity, five sets of simulations with correlation between hydraulic conductivity and porosity and two sets of simulations without between the two parameters were conducted. For the correlated case, each set consisted of three subsets with three different dispersivities. All the simulations are summarized in Table 2.2. Each set or subset of simulations consisted of two hundred heterogeneous realizations and a simulation with homogeneous hydraulic conductivity and effective porosity. In the homogeneous case, the mean values of hydraulic conductivity and effective porosity were used. By trials and errors, two hundred realizations were determined to provide reasonably stable results. The number of realizations was therefore restricted to two hundreds.

US EPA ARCHIVE DOCUMENT

Table 2.2 Statistics of Random Fields.

Correlation	Variance		Dispersivity		Case Number
	ln K	*lnϕ*	Longitudinal (m)	Transverse (m)	
Correlated	1.02	0.0014	10	0.1	C1
			50	5	C2
			100	10	C3
	2.27	0.0049	10	0.1	C4
			50	5	C5
			100	10	C6
	3.53	0.0083	10	0.1	C7
			50	5	C8
			100	10	C9
	4.80	0.0118	10	0.1	C10
			50	5	C11
			100	10	C12
	6.09	0.015	10	0.1	C13
			50	5	C14
			100	10	C15
Uncorrelated	1.02	0.0014	10	0.1	U1
	6.09	0.015	10	0.1	U2

Note: The unit of K is m/year; Mean $ln\ K = 7.55$ and Mean $ln\ \phi = -0.785$.

US EPA ARCHIVE DOCUMENT

2.3 RESULTS

2.3.1 Correlated Case

Nodal solute concentrations of each realization were normalized using the steady state solute concentrations of the homogeneous case at corresponding nodes to obtain concentration ratios. In the event that the steady-state concentration was smaller 10^{-30}, the steady-state concentration value was set to 10^{-30}. Nodal means and standard deviations of concentration ratios were obtained from the two-hundred realizations.

Figure 2.2 shows a scatter plot of the concentration ratios for the two hundred realizations at x' = x/X_w = 3.6 from the edge of the source and y' = y/X_w = 1.4 from the center of the source for case C1. X_w is the source dimension in both x and y directions (square source). Figure 2.3 presents a histogram of the logarithms of concentration ratios at the same location, along with a fitted normal curve. A normality test was conducted using the MINITAB statistical package (Minitab, 1998) and the results are shown in Figure 2.4 with a normal probability plot. Plotted in Figure 2.5 are contours of logarithms of mean concentration ratios and standard deviations of the logarithms of concentration ratios. From Figure 2.5, one can expect higher concentrations for homogeneous case than heterogeneous case if receptor well locations are located close to the plume center line. However, if receptor well locations are far from the plume center line, chances to observe higher concentrations for the heterogeneous case are higher than for the homogeneous case. The mean and standard deviation of logarithms of concentration ratios were fitted to Equation (2.3), which is a second-order model with interaction (second-order polynomial with cross terms).

$$\left[Log\left(\frac{C_{Ht}}{C_{Ho}}\right)\right]_{m,SD} = a_1 + a_2 x' + a_3 y' + a_4 x'^2 + a_5 y'^2 + a_6 x' y' \qquad (2.3)$$

where

a_1, a_2, a_3, a_4, a_5, and a_6 = the coefficients of the polynomial;

$\left[Log\left(\frac{C_{Ht}}{C_{Ho}}\right)\right]_{m,SD}$ = the mean or standard deviation of logarithms of nodal concentration ratios;

US EPA ARCHIVE DOCUMENT

US EPA ARCHIVE DOCUMENT

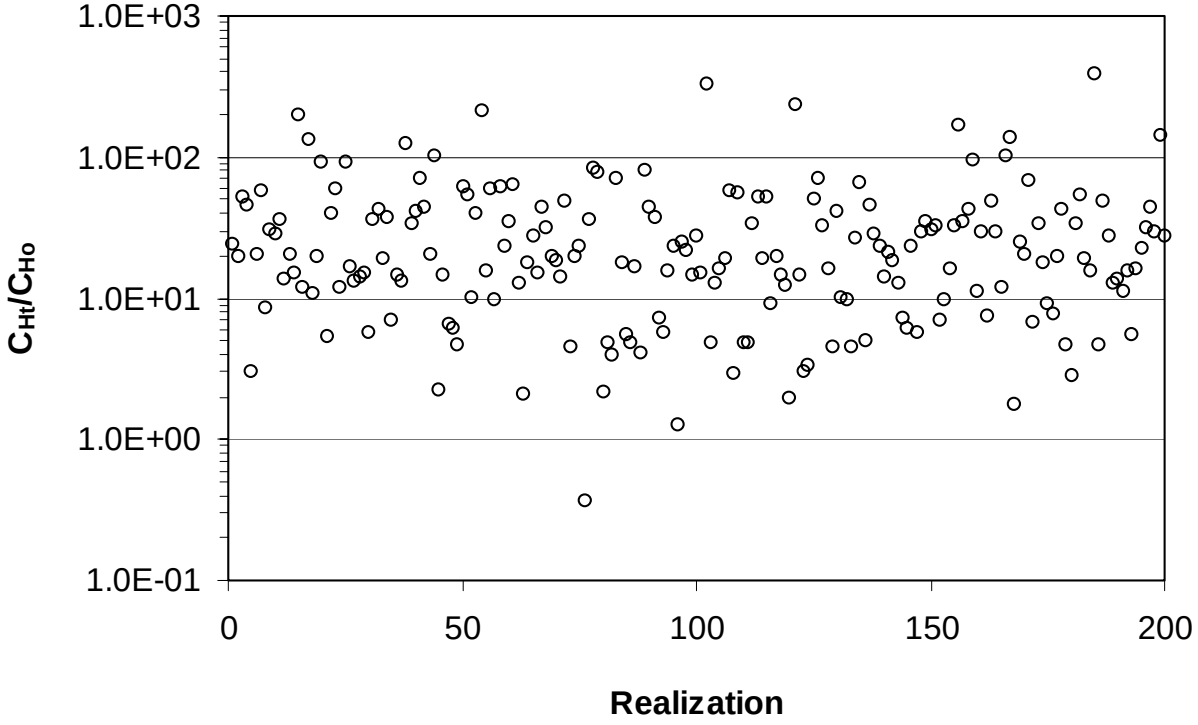

Figure 2.2 Scatter Plot of Concentration Ratios at x'=3.6 and y'=1.4.

US EPA ARCHIVE DOCUMENT

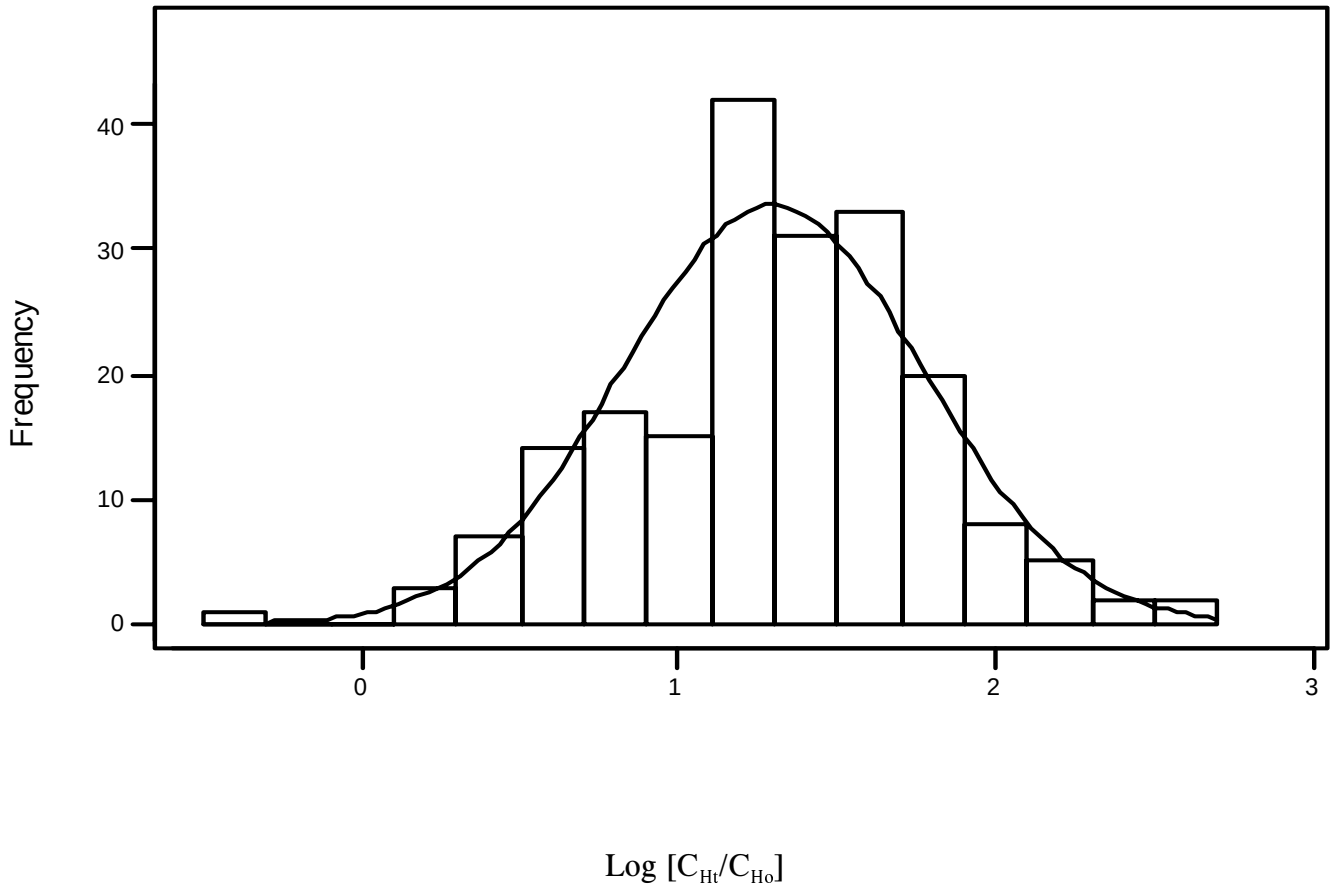

Figure 2.3 Histogram of Logarithmic Concentration Ratios with a Fitted Normal Curve at x'=3.6 and y'=1.4.

US EPA ARCHIVE DOCUMENT

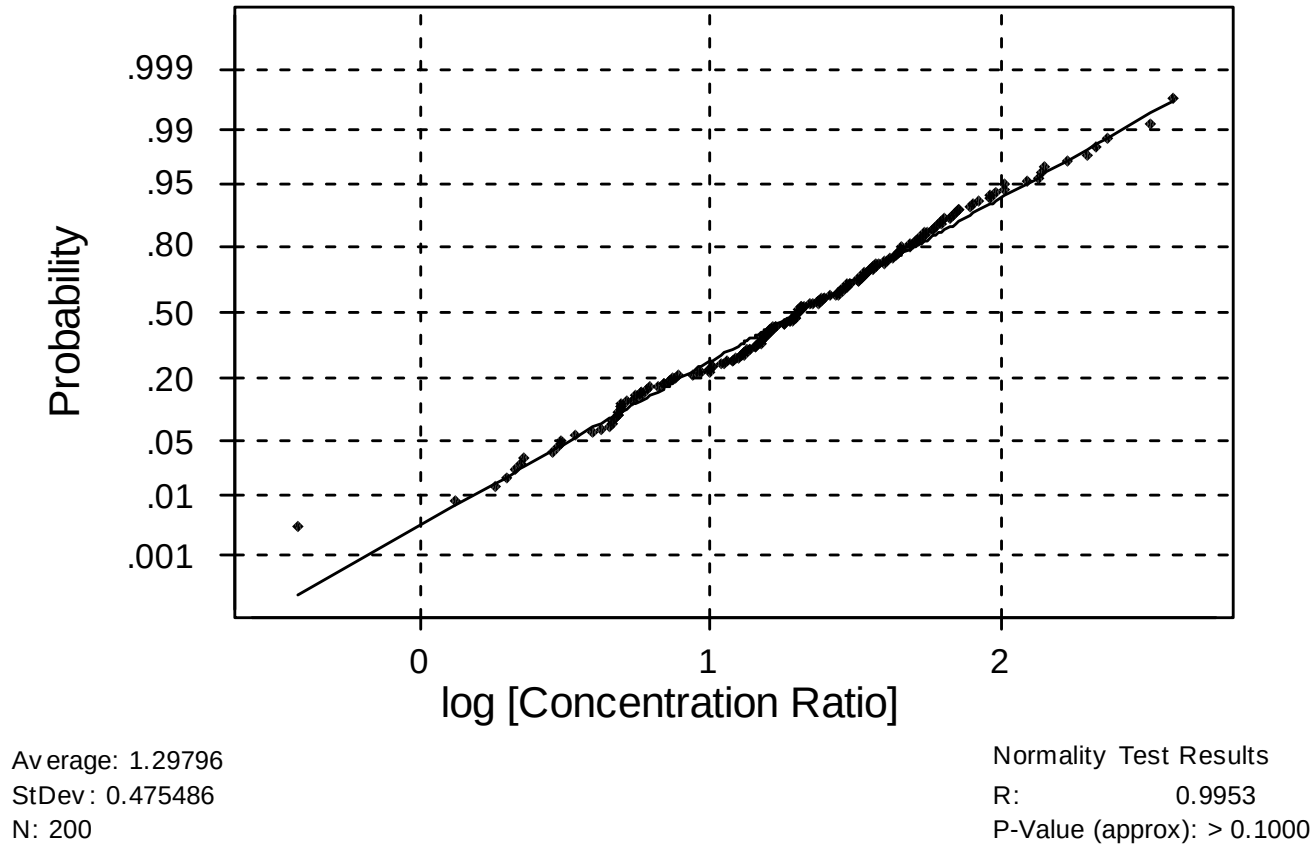

Figure 2.4 Normality Test for Logarithmic Concentration Ratio Distribution at x'=3.6 and y'=1.4.

US EPA ARCHIVE DOCUMENT

Table 2.3 Polynomial Coefficients for the correlated case

Variance of ln K	Longitudinal/ Transverse Dispersivity (m)	Variable	a_1	a_2	a_3	a_4	a_5	a_6	r^2
0.00	10/ 1	Mean	0.	0.	0.	0.	0.	0.	N/A
		Standard Dev.	0.	0.	0.	0.	0.	0.	N/A
	50/ 5	Mean	0.	0.	0.	0.	0.	0.	N/A
		Standard Dev.	0.	0.	0.	0.	0.	0.	N/A
	100/ 10	Mean	0.	0.	0.	0.	0.	0.	N/A
		Standard Dev.	0.	0.	0.	0.	0.	0.	N/A
1.02	10/ 1	Mean	-1.29E+00	1.85E-01	2.07E+00	-1.36E-02	-1.67E-02	-6.96E-02	9.60E-01
		Standard Dev.	2.11E-01	-4.47E-02	4.62E-01	-4.80E-04	-1.54E-02	-6.67E-03	9.56E-01
	50/ 5	Mean	-6.67E-02	5.43E-03	1.94E-01	-1.93E-03	1.06E-02	2.35E-03	9.96E-01
		Standard Dev.	4.47E-02	-5.97E-03	8.38E-02	-1.41E-04	-4.79E-03	-3.56E-04	9.80E-01
	100/ 10	Mean	-3.45E-02	-1.45E-03	9.57E-02	-7.11E-04	4.11E-03	1.11E-03	9.96E-01
		Standard Dev.	2.75E-02	-3.40E-03	3.71E-02	-6.07E-06	-2.35E-03	-7.55E-05	9.86E-01
2.27	10/ 1	Mean	-1.78E+00	2.88E-01	3.00E+00	-2.68E-02	2.49E-02	-7.47E-02	9.82E-01
		Standard Dev.	3.09E-01	-7.91E-02	5.66E-01	1.74E-03	-1.74E-02	-1.45E-02	9.55E-01
	50/ 5	Mean	-1.11E-01	1.18E-02	3.60E-01	-4.21E-03	1.93E-02	5.15E-03	9.94E-01
		Standard Dev.	7.40E-02	-8.34E-03	1.08E-01	-2.86E-04	-6.31E-03	-3.30E-04	9.76E-01
	100/ 10	Mean	5.31E-02	-2.61E-03	1.79E-01	-1.59E-03	7.86E-03	2.56E-03	9.94E-01
		Standard Dev.	4.67E-02	-4.83E-03	4.93E-02	-6.59E-05	-3.34E-03	3.08E-05	9.82E-01
3.53	10/ 1	Mean	-1.90E+00	3.20E-01	3.32E+00	-3.21E-02	5.25E-02	-7.82E-02	9.85E-01
		Standard Dev.	3.69E-01	-9.75E-02	6.01E-01	3.01E-03	-1.52E-02	-1.97E-02	9.54E-01
	50/ 5	Mean	-1.23E-01	1.50E-02	4.28E-01	-5.34E-03	2.36E-02	6.25E-03	9.93E-01
		Standard Dev.	9.36E-02	-1.03E-02	1.19E-01	-3.16E-04	-7.04E-03	-3.59E-04	9.74E-01
	100/ 10	Mean	-5.35E-02	-2.96E-03	2.12E-01	-2.05E-03	9.70E-03	3.29E-03	9.94E-01
		Standard Dev.	5.99E-02	-5.80E-03	5.52E-02	-1.05E-04	-3.90E-03	1.50E-04	9.78E-01

US EPA ARCHIVE DOCUMENT

4.80	10/ 1	Mean	-1.95E+00	3.28E-01	3.52E+00	-3.40E-02	7.18E-02	-8.46E-02	9.86E-01
		Standard Dev.	4.09E-01	-1.11E-01	6.27E-01	4.04E-03	-1.39E-02	-2.36E-02	9.55E-01
	50/ 5	Mean	-1.26E-01	1.66E-02	4.66E-01	-6.01E-03	2.66E-02	6.76E-03	9.93E-01
		Standard Dev.	1.10E-01	-1.20E-02	1.28E-01	-3.20E-04	-7.52E-03	-4.60E-04	9.72E-01
	100/ 10	Mean	-4.90E-02	-3.27E-03	2.30E-01	-2.32E-03	1.09E-02	3.75E-03	9.93E-01
		Standard Dev.	7.08E-02	-6.53E-03	5.98E-02	-1.39E-04	-4.29E-03	2.33E-04	9.75E-01
6.09	10/ 1	Mean	-1.99E+00	3.25E-01	3.65E+00	-3.42E-02	8.73E-02	-9.20E-02	9.86E-01
		Standard Dev.	4.40E-01	-1.21E-01	6.49E-01	4.83E-03	-1.32E-02	-2.67E-02	9.57E-01
	50/ 5	Mean	-1.26E-01	1.71E-02	4.91E-01	-6.41E-03	2.90E-02	6.95E-03	9.92E-01
		Standard Dev.	1.24E-01	-1.35E-02	1.35E-01	-3.15E-04	-7.87E-03	-5.98E-04	9.71E-01
	100/ 10	Mean	-4.32E-01	3.64E-02	2.40E-01	-2.50E-03	1.19E-02	4.06E-03	9.93E-01
		Standard Dev.	8.10E-01	-7.28E-02	6.36E-01	-1.58E-04	-4.59E-03	-2.85E-04	9.73-01

12

Table 2.4 Polynomial Coefficients for the uncorrelated case

Variance	Longitudinal/ Transverse Dispersivity (m)	Variable	a_1	a_2	a_3	a_4	a_5	a_6	r^2
1.02	10/ 1	Mean	-1.25E+00	1.99E-01	2.00E+00	-1.53E-02	-2.36E-02	-6.56E-02	95.5
		Standard Dev.	1.41E-01	-1.69E-02	4.25E-01	-2.46E-03	-1.04E-02	-5.32E-03	95.6
6.09	10/ 1	Mean	-1.93E+00	3.36E-01	3.53E+00	-3.54E-02	6.87E-02	-8.17E-02	98.6
		Standard Dev.	2.98E-01	-6.58E-02	5.78E-01	7.51E-04	-3.99E-03	-2.32E-02	95.7

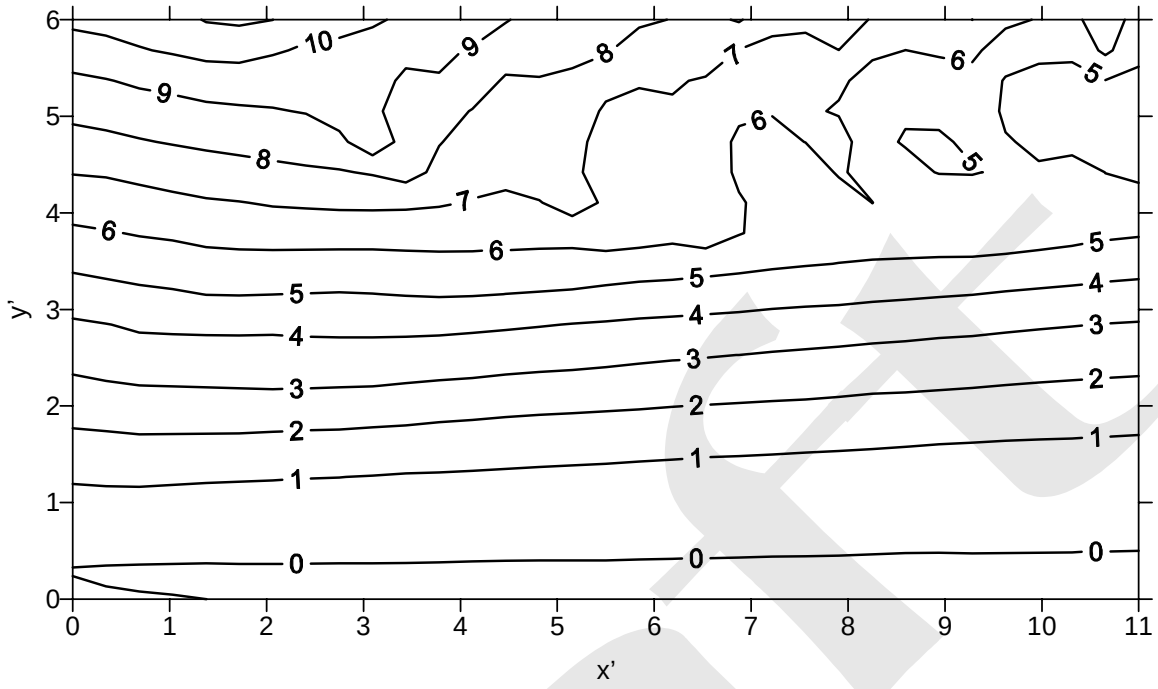

2.5 (a)

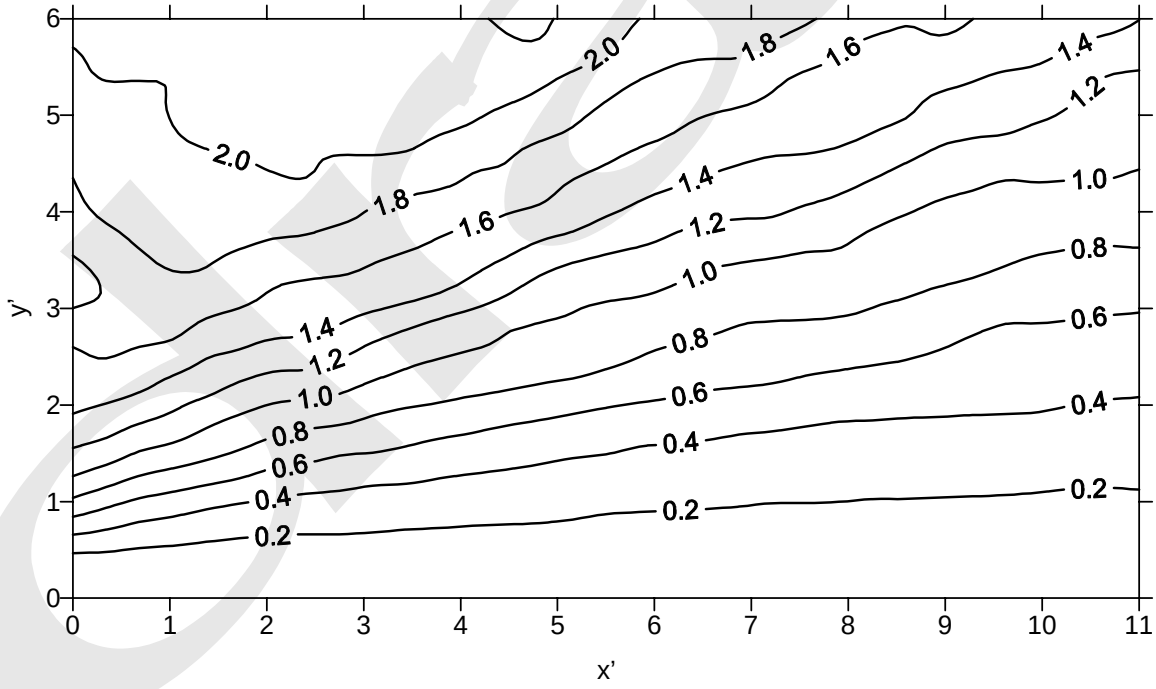

2.5 (b)

Figure 2.5 Contours of (a) Mean Logarithmic Concentration Ratios and (b) Standard Deviations of Logarithmic Concentration Ratios for Case C1.

US EPA ARCHIVE DOCUMENT

US EPA ARCHIVE DOCUMENT

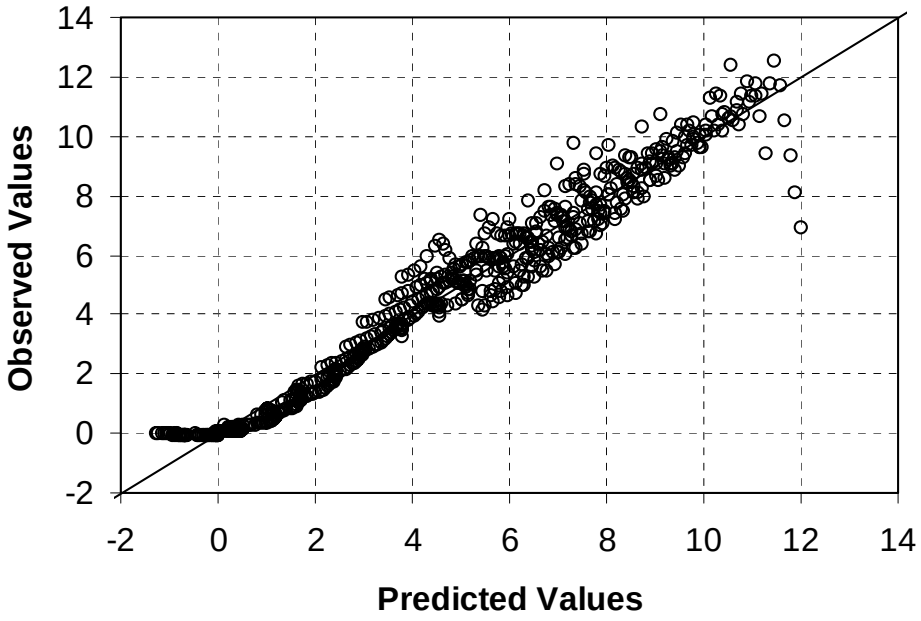

2.6 (a)

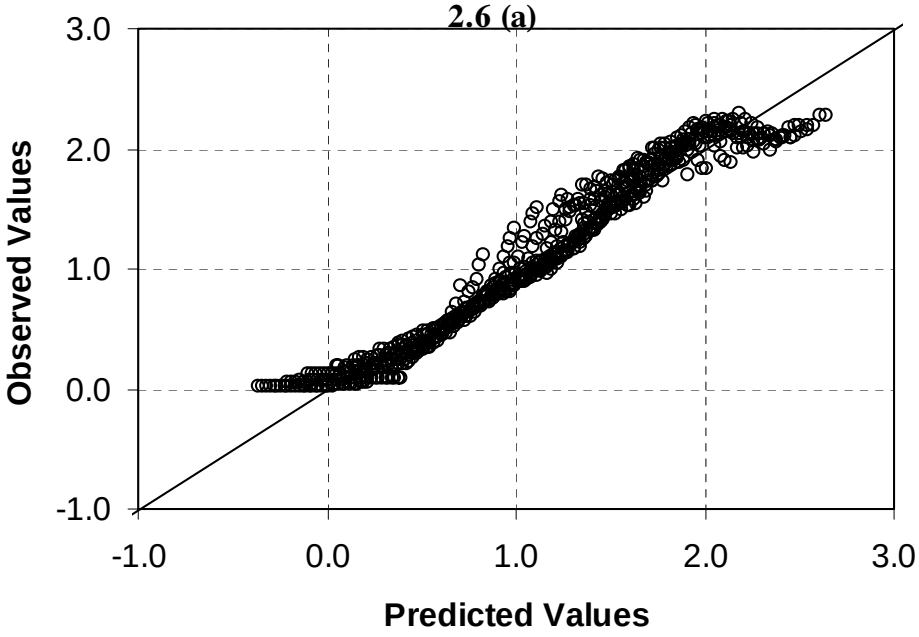

2.6 (b)

Figure 2.6 Observed vs. Predicted Values of (a) Mean Logarithmic Concentration Ratios and (b) Standard Deviations of Logarithmic Concentration Ratios for Case C1.

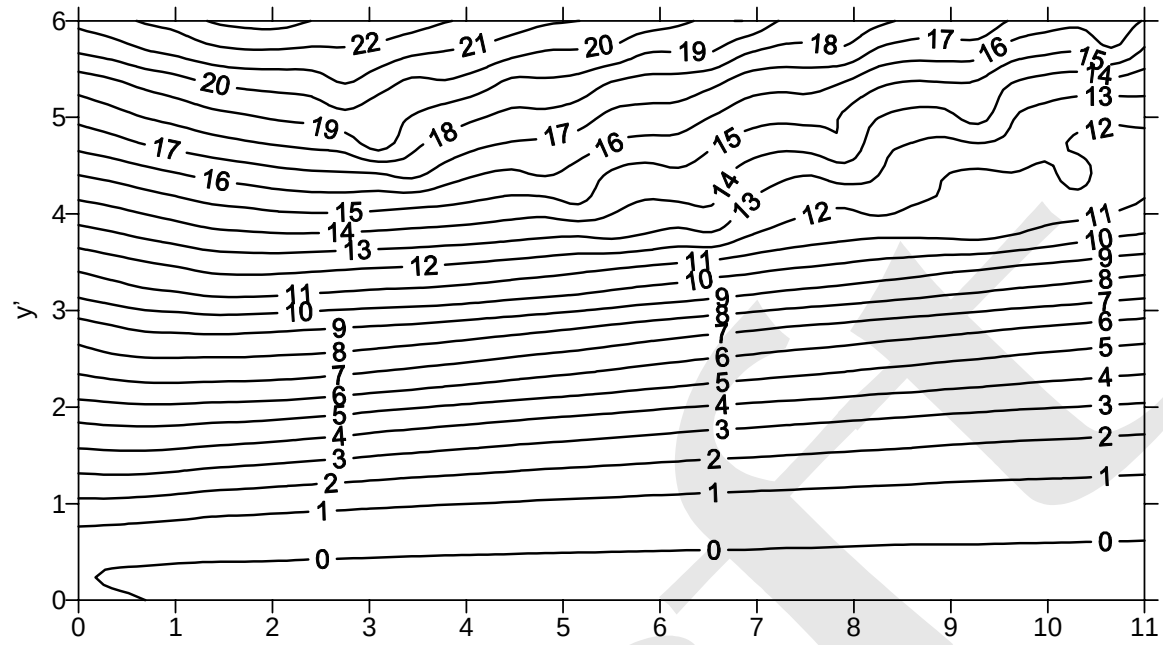

2.7 (a)

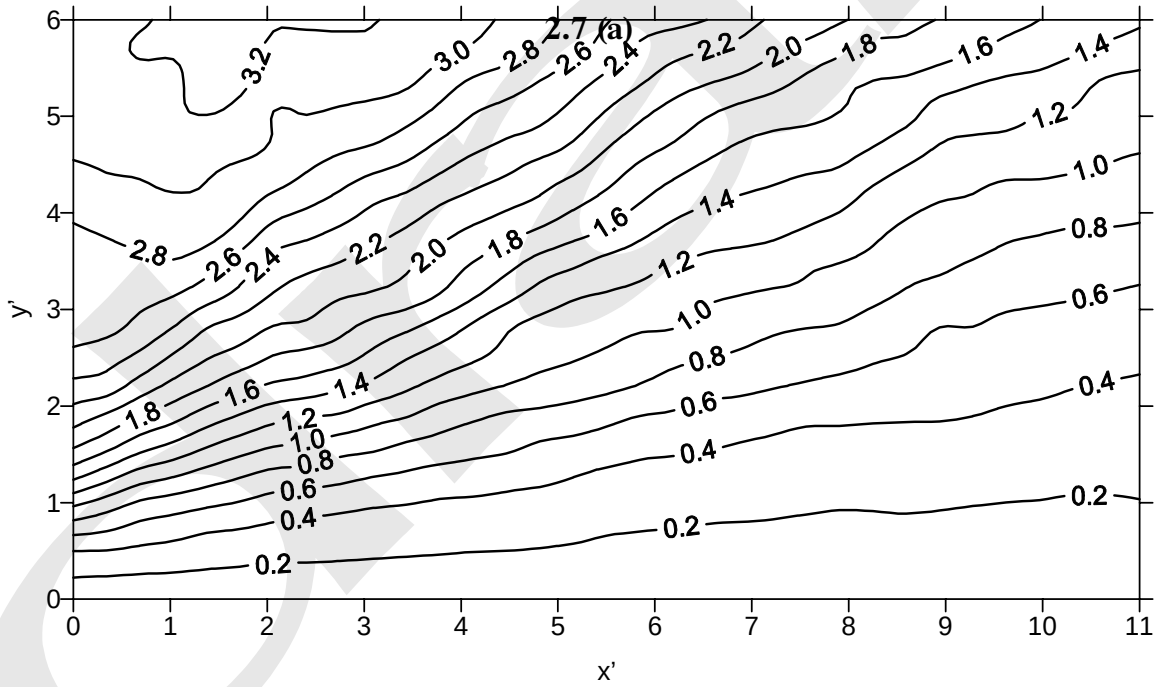

2.7 (b)

Figure 2.7 **Contours of (a) Mean Logarithmic Concentration Ratios and (b) Standard Deviations of Logarithmic Concentration Ratios for Case C13.**

US EPA ARCHIVE DOCUMENT

US EPA ARCHIVE DOCUMENT

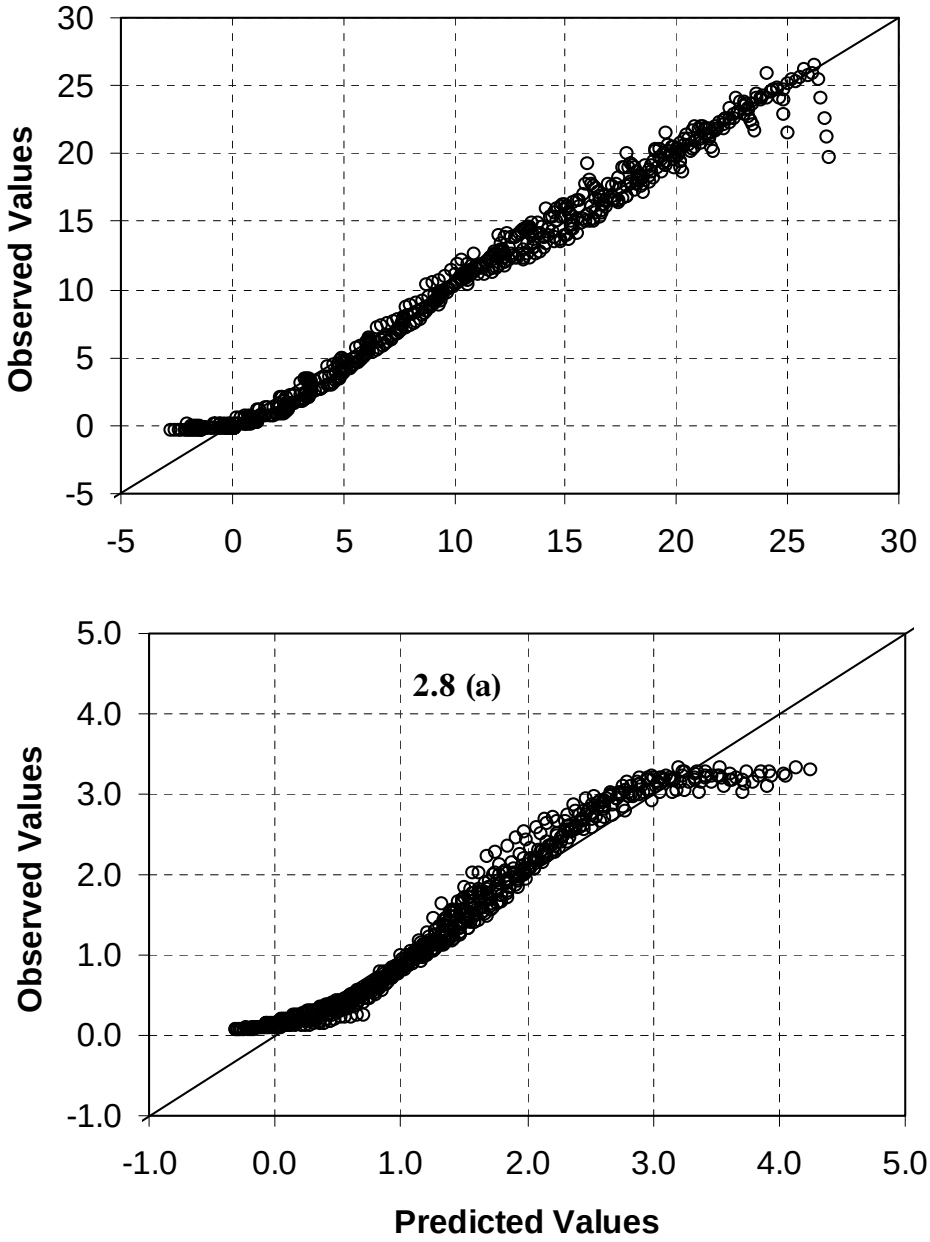

Figure 2.8 **Observed vs. Predicted Values of (a) Mean Logarithmic Concentration Ratios and (b) Standard Deviations of Logarithmic Concentration Ratios for Case C13.**

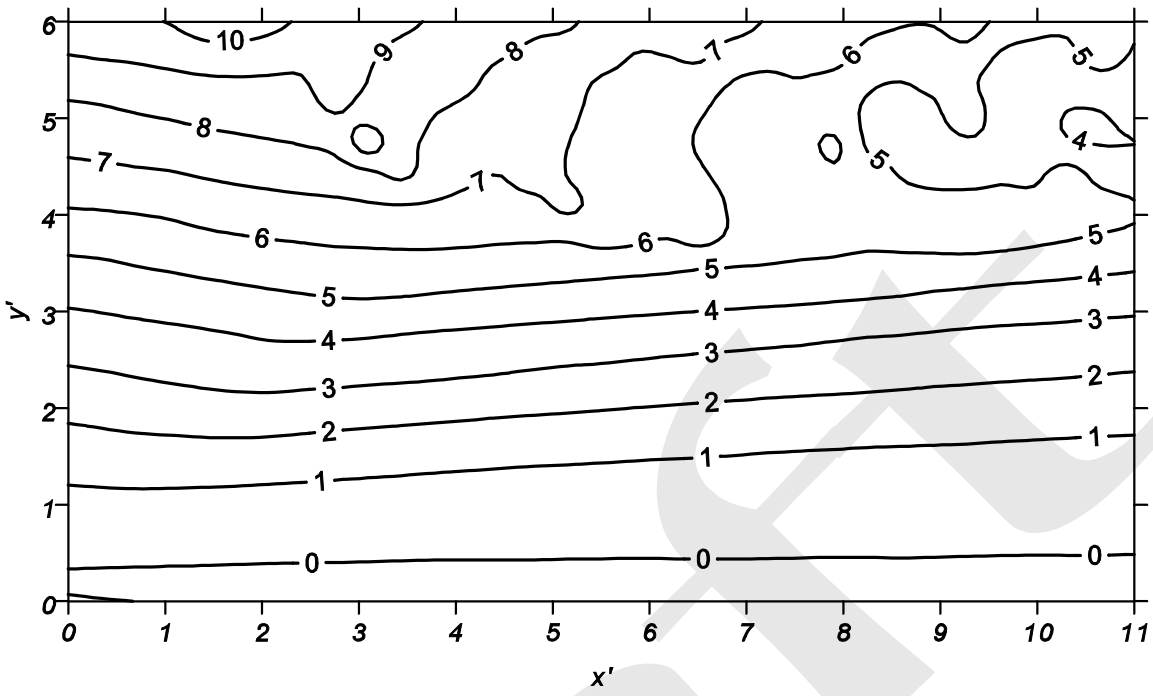

2.9 (a)

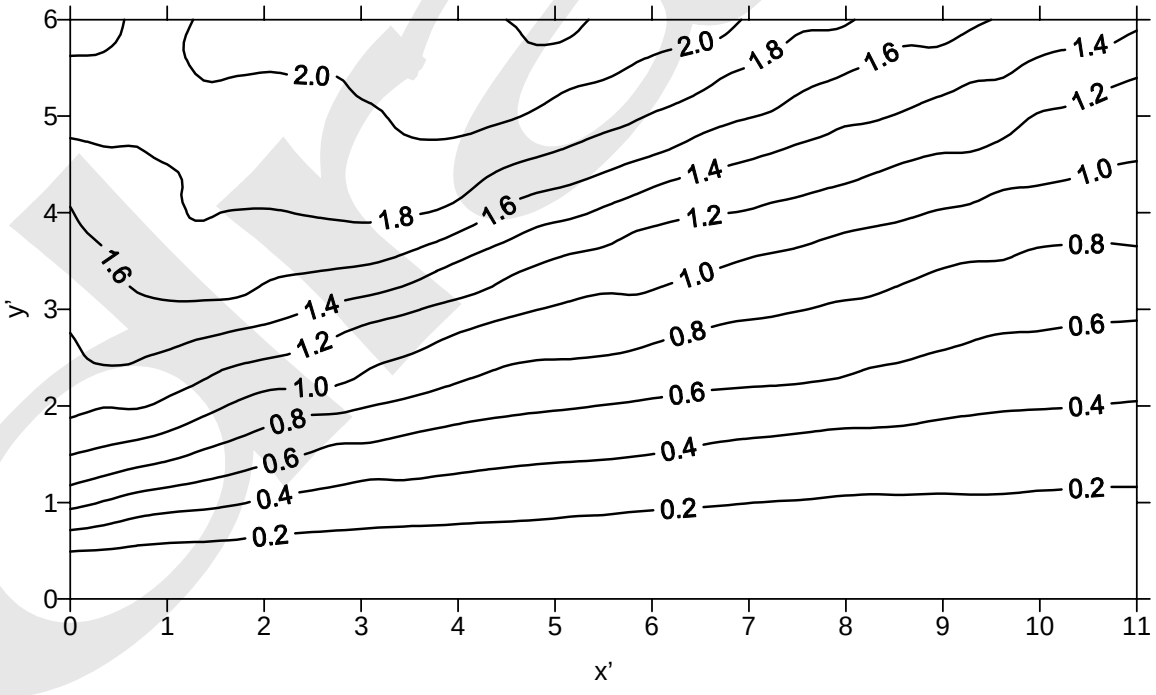

2.9 (b)

Figure 2.9 Contours of (a) Mean Logarithmic Concentration Ratios and (b) Standard Deviations of Logarithmic Concentration Ratios for Case U1.

US EPA ARCHIVE DOCUMENT

US EPA ARCHIVE DOCUMENT

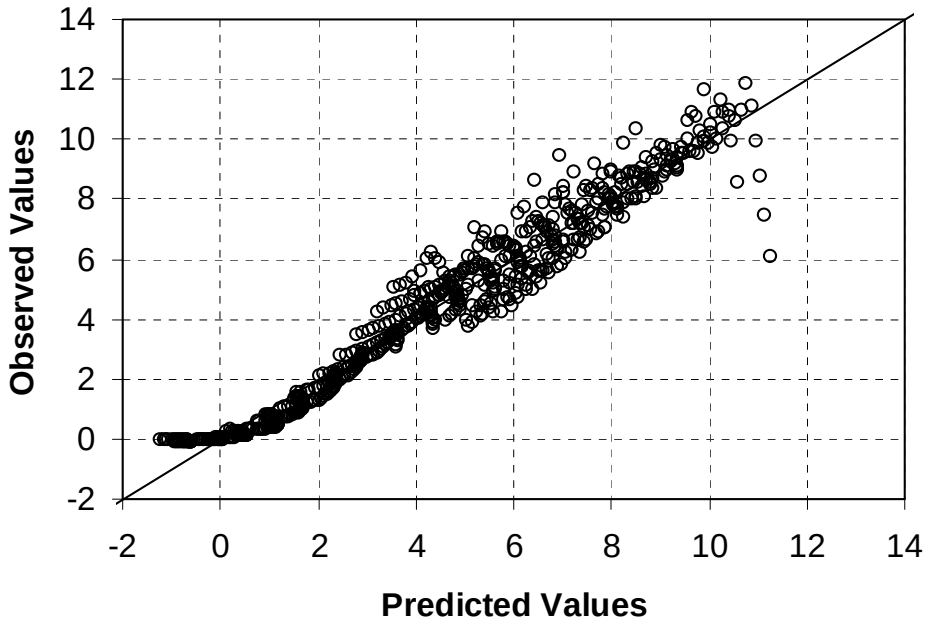

2.10 (a)

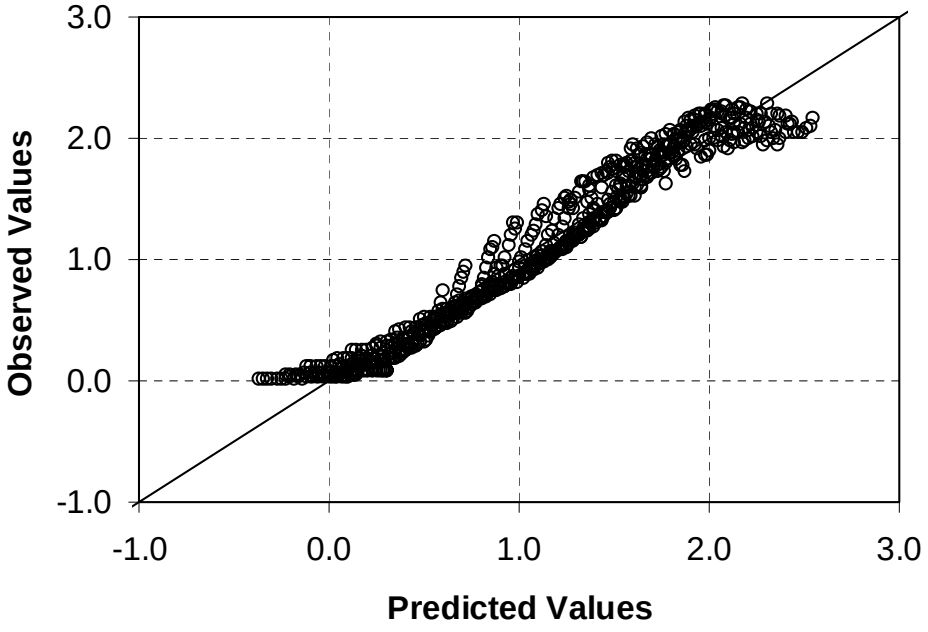

2.10 (b)

Figure 2.10 Observed vs. Predicted Values of (a) Mean Logarithmic Concentration Ratios and (b) Standard Deviations of Logarithmic Concentration Ratios for Case U1.

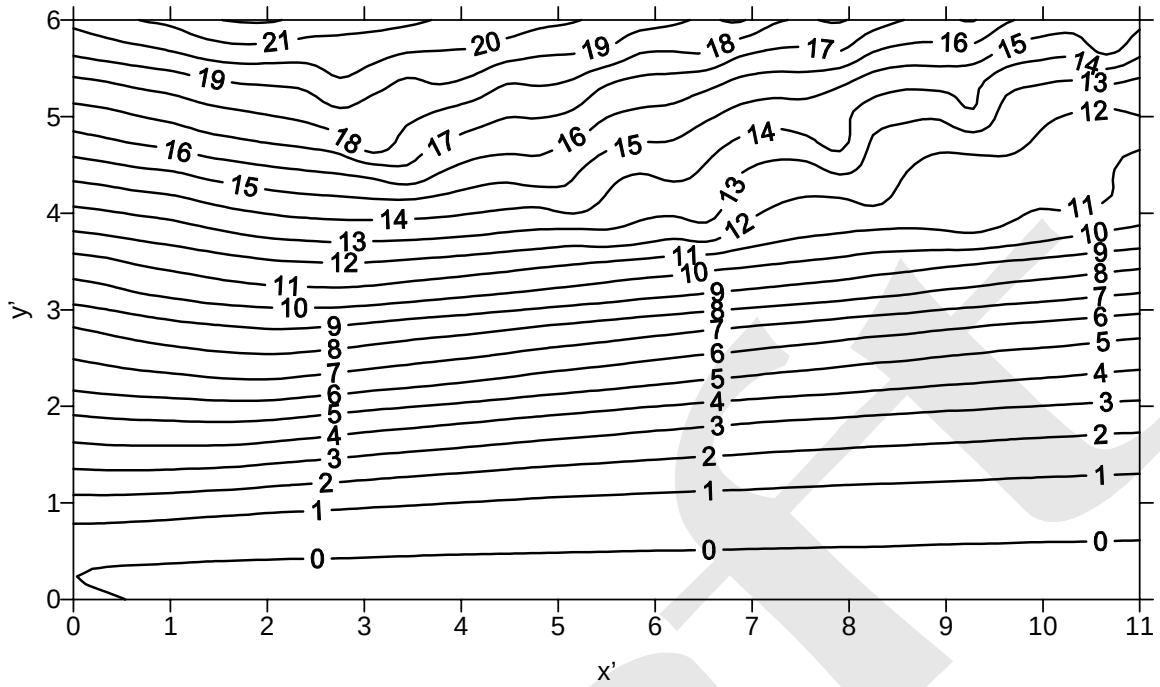

2.11 (a)

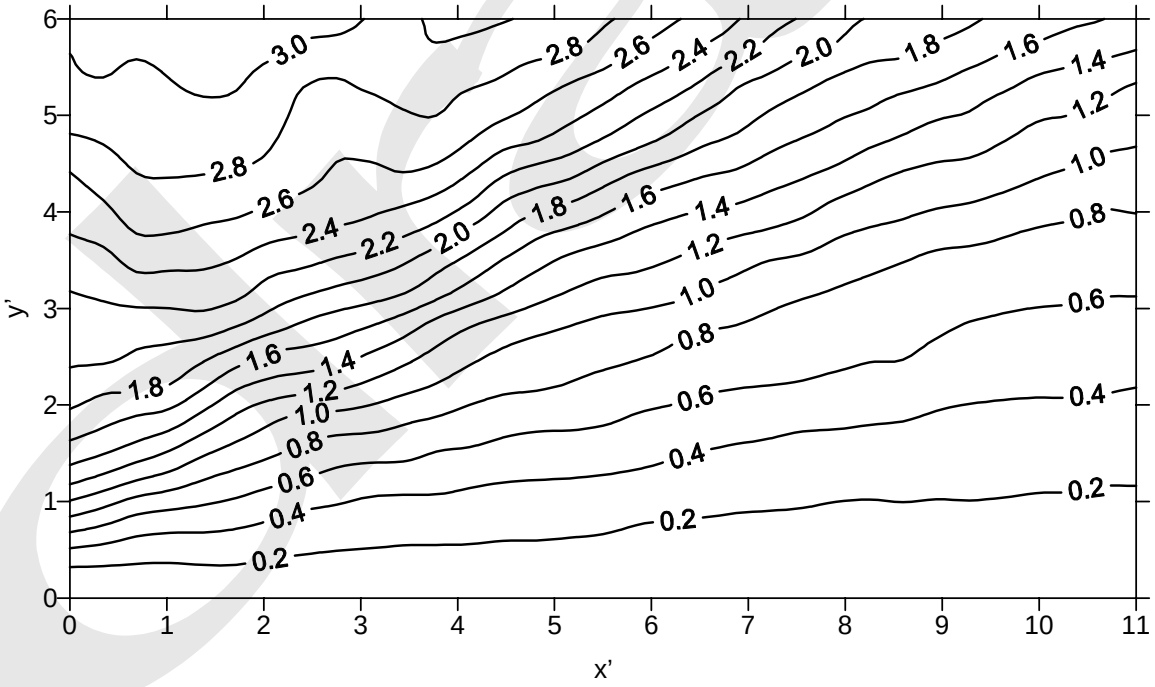

2.11 (b)

Figure 2.11 Contours of (a) Mean Logarithmic Concentration Ratios and (b) Standard Deviations of Logarithmic Concentration Ratios for Case U2.

US EPA ARCHIVE DOCUMENT

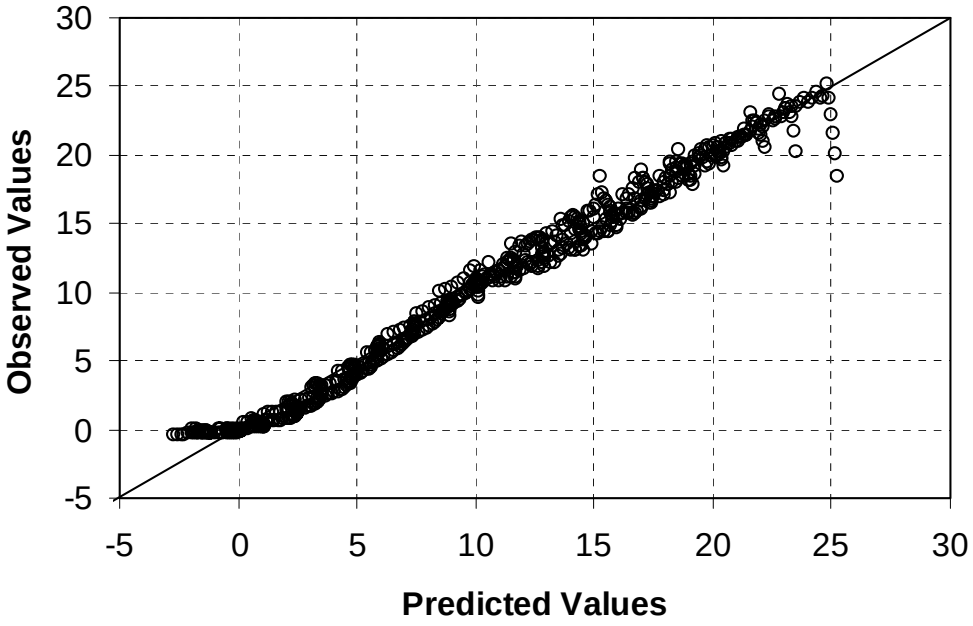

2.12 (a)

US EPA ARCHIVE DOCUMENT

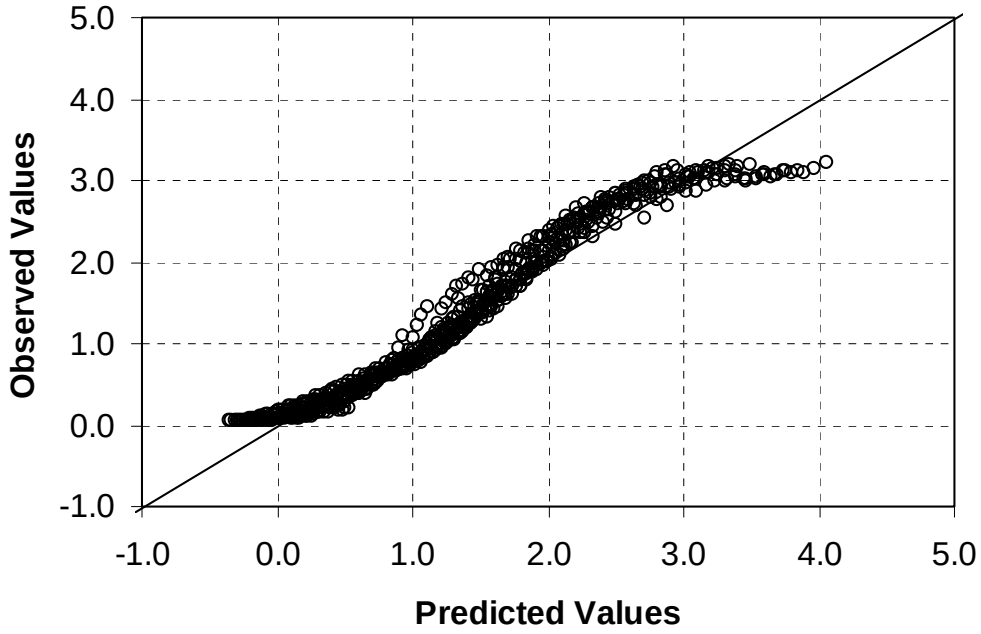

2.12 (b)

Figure 2.12 Observed vs. Predicted Values of (a) Mean Logarithmic Concentration Ratios and (b) Standard Deviations of Logarithmic Concentration Ratios for Case U2.

US EPA ARCHIVE DOCUMENT

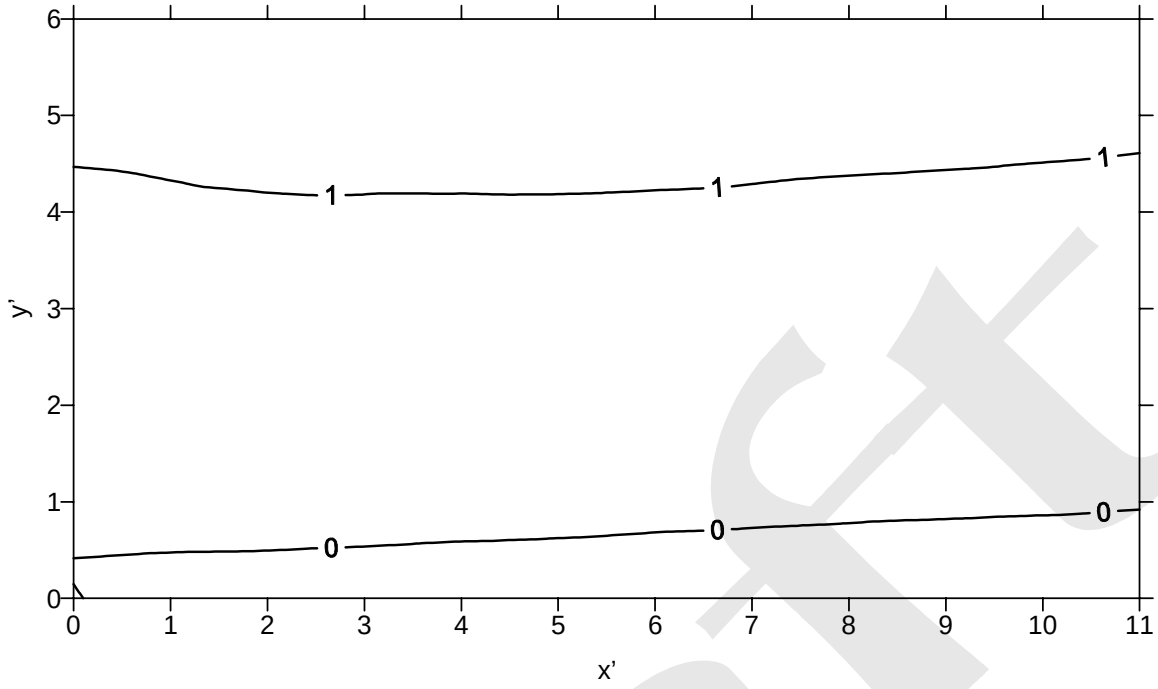

2.13 (a)

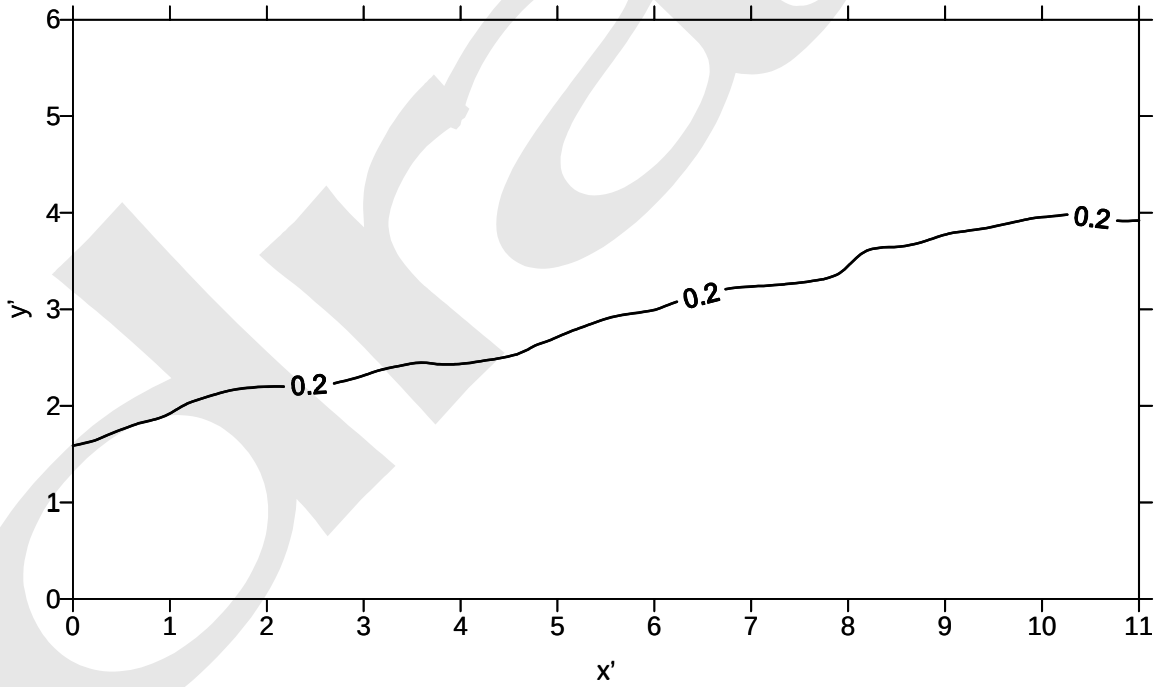

2.13 (b)

Figure 2.13 Contours of (a) Mean Logarithmic Concentration Ratios and (b) Standard Deviations of Logarithmic Concentration Ratios for Case C2.

US EPA ARCHIVE DOCUMENT

draft

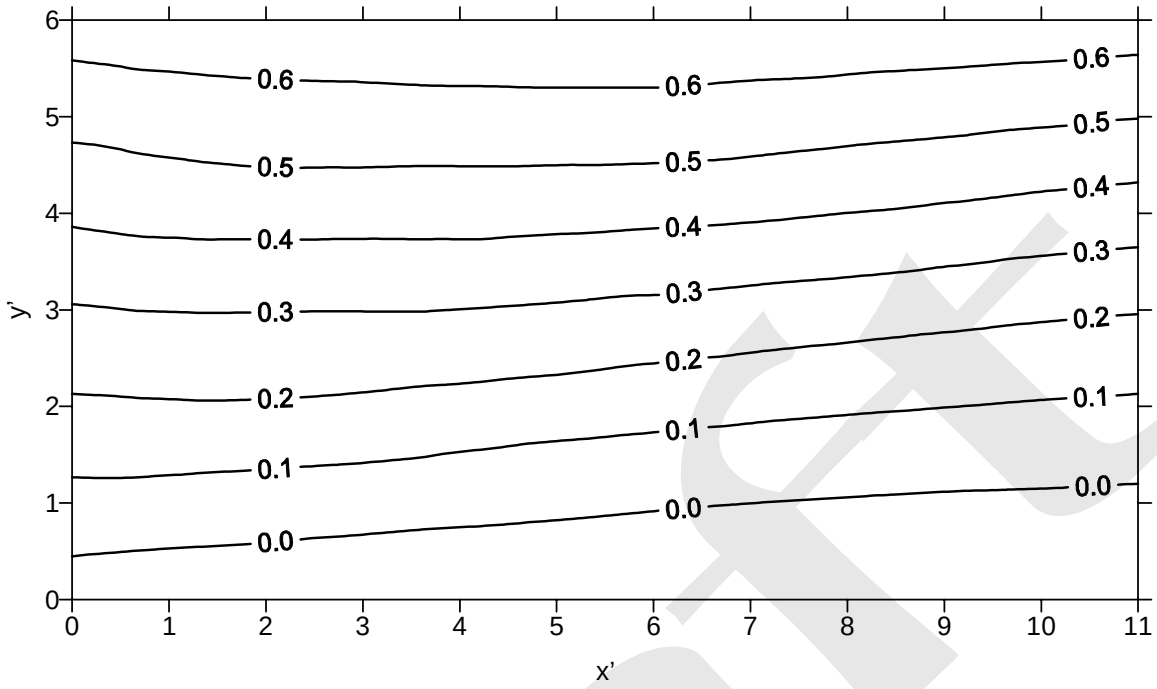

2.14 (a)

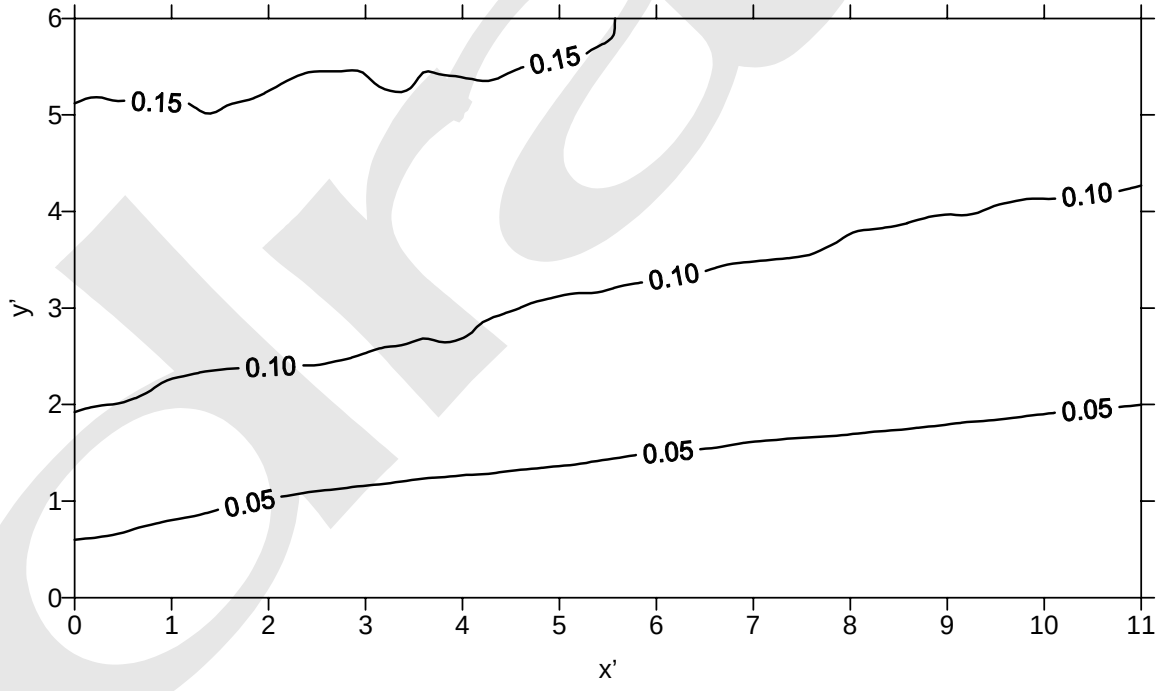

2.14 (b)

Figure 2.14 Contours of (a) Mean Logarithmic Concentration Ratios and (b) Standard Deviations of Logarithmic Concentration Ratios for Case C3.

US EPA ARCHIVE DOCUMENT

draft

C_{Ht}	=	The nodal concentration from simulation with heterogeneous materials; and
C_{Ho}	=	The nodal concentration from simulation with homogeneous materials.

The coefficients were determined by a multiple-regression analysis using the STATISTICA statistical software package (Statsoft, 1993). Figure 2.6a shows a comparison between the observed and predicted values (by the polynomial). All the coefficients are listed in Table 2.3. Fitting for standard deviations are shown in Figure 2.6b and the coefficients are also listed in Table 2.3. In Figure 2.6 it may be observed that the majority of the mean and standard aviation values may be accurately predicted of the polynomials.

The effects of the degree of heterogeneity were further evaluated by increasing the variances of *ln* ϕ and *ln K* by up to an order of magnitude as shown in Table 2.2. The contours of mean logarithmic concentration ratios and standard deviations of the logarithmic concentration ratios for case C13 are presented in Figure 2.7 and the contours for the intermediate variances of *ln* ϕ and *ln K* are presented in Appendix A. As seen in Figure 2.7, the increased variances in *ln* ϕ and *ln K* significantly affected the distributions of the mean logarithmic concentration ratios and the standard deviations of logarithmic concentration ratios. Presented in Figure 2.8 are the observed versus predicted mean logarithmic concentration ratios and the standard deviations of logarithmic concentration ratios for Case 13. All the coefficients are listed in Table 2.3.

2.3.2 Uncorrelated Case

Two simulations (U1 and U2) were conducted to evaluate the effects associated with correlation between logarithmic hydraulic conductivity and porosity. Results are presented in Figures 2.9 to 2.12. Figure 2.9 shows the contours of mean logarithmic concentration ratios and standard deviations of logarithmic concentration ratios for the small variances of *ln* ϕ and *ln K* for the uncorrelated case (Case U1), which are very similar to the results obtained for the same variances of the correlated case presented in Figure 2.5. Figure 2.10 presents the observed versus predicted values for mean logarithmic concentration ratios and standard deviations of logarithmic concentration ratios for Case U1. All the coefficients for the uncorrelated case are listed in Table 2.4. Presented in Figure 2.11 are the contours of mean logarithmic concentration ratios and standard deviations of the logarithmic concentration ratios for the large variances of *ln* ϕ and *ln K* (Case U2). Similar to the results from the correlated case, the increased variances in *ln* ϕ and *ln K* significantly affected the distributions of the mean logarithmic concentration ratios and the standard deviations of logarithmic concentration ratios. Presented in Figure 2.12 are the observed versus predicted mean logarithmic concentration ratios and the standard deviations of logarithmic concentration ratios for Case U2.

In general, the results based on correlated logarithmic conductivity and porosity are similar to those without correlation. Additionally, correlation between logarithmic conductivity and porosity

US EPA ARCHIVE DOCUMENT

is more consistent with physical observation. The case of uncorrelated logarithmic conductivity and porosity was not further investigated.

2.3.3 Dispersivity Effects

Figure 2.13 and 2.14 show the contours of mean logarithmic concentration ratios and standard deviations of logarithmic concentration ratios for Cases C2 and C3 using two dispersivity values of 50 and 100 m, respectively. These two values in addition to 10 m were selected to take into account effects of different dispersivity values in Monte Carlo simulations as presented in section 3. Note that the transverse dispersivity values are 10 percent of the longitudinal dispersivity values. Results for other variances of *ln* ϕ and *ln K* using longitudinal dispersivity values of 50 and 100 m are presented in Appendix A. Fitting coefficients are listed in Table 2.3. As seen in Figures 2.13 and 2.14, increased dispersivity resulted in significant decrease of mean logarithmic concentration ratios and standard deviations of logarithmic concentration ratios in the simulation domain. As dispersivity becomes increasingly large, both the mean and standard deviation of the logarithmic concentrations approach 0 due to the increase of hydrodynamic dispersion.

2.4 TREATMENT OF HETEROGENEITY

In the previous sections, it has been shown that concentration ratios are log-normally distributed. Alternatively, it can be stated that:

$$\ln(C_{Ht}) = \ln(C_{Ho}) + \mu + N(0,\sigma) \qquad \textbf{(2.4)}$$

μ = $\mu\left(x, y, \alpha_T, Var(ln\ K)\right)$

= Mean of natural logarithmic concentration ratio

σ = $\sigma\left(x, y, \alpha_T, Var(ln\ K)\right)$

= Standard deviation of natural logarithmic concentration ratio

Note that the mean and standard deviation of the logarithmic concentration ratios are expressed in terms of transverse dispersivity instead of longitudinal dispersivity. For steady-state transport with a source of finite dimension, it has been shown that the longitudinal dispersion terms in the transport equation are negligible compared with the transverse dispersion terms and may be omitted from the transport equation without causing significant errors (Harleman and Rumer, 1963). Transverse dispersivity values in porous materials are normally expressed as fractions of longitudinal dispersivity values.

In Equation (2.4), the first two terms on the right hand side represent a redistribution of mean concentration due to the presence of heterogeneity in the transport domain. The redistribution of

US EPA ARCHIVE DOCUMENT

mass is similar to the effects due to an increase in transverse dispersion. In this document, the increase in transverse dispersion due to heterogeneity is referred to as macro-dispersion. The last term represents local stochastic fluctuation of concentration, or perturbation of concentration. One can see that the effects due to heterogeneity may be divided into two components: the macro-dispersion effects, described by μ; and the local stochastic fluctuation about the mean concentration associated with spatially varied hydraulic conductivity, described by σ. The macro-dispersion effects include the effects due to both the local dispersivity and the heterogeneity of the hydraulic conductivity. In the previous sections, it has also been observed that μ and σ approach 0, as α_L and α_T become increasingly large. Therefore, the macro-scale dispersion effects and local stochastic fluctuation due to the variability of hydraulic conductivity diminish with the increase of local-scale dispersivity values.

Because the first two terms on the right hand side of Equation (2.4) comprise the combination of macro-dispersion and local dispersion effects (or total dispersion), the equation may be recast as:

$$\ln C_{Ht} = \ln C_{Ho}^{*} + N(0,\sigma) \qquad \textbf{(2.5)}$$

where

C_{Ho}^{*} = Concentration computed by a modified homogeneous model with the total transverse dispersivity.

The macro-dispersivity may be given as a function of *Var* (ln *K*) (Gelhar, 1993), thus:

$$\alpha_T^M = \beta Var(\ln K) \qquad \textbf{(2.6)}$$

In Equation (2.6), β is a parameter that relates *Var* (ln *K*) to macro-dispersivity. Assuming that the total dispersivity is a linear combination between macro-dispersivity and local dispersivity, the total transverse dispersivity is given by:

$$\alpha_T^{Tot} = \alpha_T + \alpha_T^M \qquad \textbf{(2.7)}$$

The two-dimensional steady-state transport equation for a conservative solute may be written as (Gelhar, 1993):

$$Q_x \frac{\partial C_{Ho}^{*}}{\partial x} = (\alpha_T + \alpha_T^M) Q_x \frac{\partial}{\partial y}\left(\frac{\partial C_{Ho}^{*}}{\partial y}\right) \qquad \textbf{(2.8)}$$

US EPA ARCHIVE DOCUMENT

where

Q_x	=	Spatially invariant mean Darcy velocity in the x direction
x	=	Distance along the flow direction from the downgradient boundary of the waste management unit
y	=	Distance normal to the flow direction from the center line of the waste management unit.

Note that in Equation (2.8), the longitudinal dispersion term is omitted. In addition, the equation is based on the following conditions:

$$\begin{aligned} q_x &= Q_x + q_x' \\ q_y &= Q_y + q_y' \\ E[q_x'] &= 0 \\ Q_y &= 0 \\ E[q_y'] &= 0 \end{aligned} \qquad \textbf{(2.9)}$$

where

q_x	=	Spatially varied Darcy velocity in the x direction
q'_x	=	Perturbation of Darcy velocity in the x direction
Q_y	=	Invariant Mean Darcy velocity in the y direction
q_y	=	Spatially varied Darcy velocity in the y direction
q'_y	=	Perturbation of Darcy velocity in the y direction
E[·]	=	Expectation operator.

Using Equations (2.6) and (2.7), Equation (2.8) may be presented in a normalized form as follows:

$$\frac{\partial C^{*\prime}}{\partial x'} = \left(\frac{\alpha_T}{X_W} + \frac{\beta}{X_W} Var(\ln K) \right) \frac{\partial}{\partial y'} \left(\frac{\partial C^{*\prime}}{\partial y'} \right) \qquad \textbf{(2.10)}$$

where:

$C^{*'}$	=	C/C_{oRef}
C_{oRef}	=	Reference concentration
x'	=	x/X_{WRef}
y'	=	y/X_{WRef}
X_{WRef}	=	Reference waste management (square) unit side dimension (both width and length).

Equation (2.5) can be restated as:

US EPA ARCHIVE DOCUMENT

$$\ln\frac{C_{Ht}}{C_{oSite}} = \ln\frac{C^{*}_{Ho}}{C_{oSite}} + \ln \varpi^{*}_{Ho} \qquad \textbf{(2.11)}$$

where ϖ_{Ho}^{*} = Perturbation of concentration ratio associated with the modified homogeneous model with total transverse dispersion

C_{oSite} = Reference concentration at the site.

From Equation (2.10), it can be stated that for a site subject to similar conditions, the concentration at location x', y' may be determined from:

$$\begin{aligned} & C^{*}_{HoSite}\left(x', y', \frac{\beta_{Site}}{X_{WSite}}, \frac{\alpha_{TSite}}{X_{WSite}}, Var(\ln K)_{Site}\right) \\ = \; & \frac{C_{oSite}}{C_{oRef}} C^{*}_{Ref}\left(x', y', \frac{\beta_{Ref}}{X_{WRef}}, \frac{\alpha_{TRef}}{X_{WRef}}, Var(\ln K)_{Ref}\right) \end{aligned} \qquad \textbf{(2.12)}$$

It follows that, in a statistical sense, the corresponding perturbation of concentration ratio may be determined from:

$$\begin{aligned} & \varpi^{*}_{HoSite}\left(x', y', \frac{\beta_{Site}}{X_{WSite}}, \frac{\alpha_{TSite}}{X_{WSite}}, Var(\ln K)_{Site}\right) \\ = \; & \varpi^{*}_{Ref}\left(x', y', \frac{\beta_{Ref}}{X_{WRef}}, \frac{\alpha_{TRef}}{X_{WRef}}, Var(\ln K)_{Ref}\right) \end{aligned} \qquad \textbf{(2.13)}$$

In the above two equations, parameters with the extended subscripts *Ref* and *Site* are the reference and site parameters, respectively. The reference parameters are those used in Table 2.3.

The parameter β is normally expressed as a function of local dispersivities (Gelhar, 1993). In the following analysis, it is assumed that if:

$$\frac{\alpha_{TSite}}{X_{WSite}} = \frac{\alpha_{TRef}}{X_{WRef}} \qquad \textbf{(2.14a)}$$

then, the following condition is automatically true,

US EPA ARCHIVE DOCUMENT

$$\frac{\beta_{Site}}{X_{WSite}} = \frac{\beta_{Ref}}{X_{WRef}} \quad \textbf{(2.14b)}$$

From Equations (2.4), (2.5), and (2.10) to (2.14), it can be stated that:

$$\mu_{Site}(x', y', \frac{\alpha_{TSite}}{X_{WSite}}, Var(\ln K)_{Site}) = \mu_{Ref}(x', y', \frac{\alpha_{TRef}}{X_{WRef}}, Var(\ln K)_{Ref}) \quad \textbf{(2.15)}$$

and that:

$$\sigma_{Site}(x', y', \frac{\alpha_{TSite}}{X_{WSite}}, Var(\ln K)_{Site}) = \sigma_{Ref}(x', y', \frac{\alpha_{TRef}}{X_{WRef}}, Var(\ln K)_{Ref}) \quad \textbf{(2.16)}$$

Using Equation (2.4) with the mean and standard deviation given in Equations (2.15), and (2.16), realizations of steady-state contaminant concentration at any given location x', y' may be generated. The reference mean and standard deviation in Equations (2.15) and (2.16) may be obtained using Equation (2.3) and coefficients in Table 2.3. Interpolation between neighboring points may be necessary.

It should be noted that the analysis has been conducted for the case of steady-state transport. For the case of transient transport, it is assumed that the concentration difference between the heterogeneous and the corresponding homogeneous settings is time-invariant and equal to the corresponding steady-state cases.

US EPA ARCHIVE DOCUMENT

draft

US EPA ARCHIVE DOCUMENT

3.0 HETEROGENEITY IN SIMULATIONS BY EPACMTP

3.1 TREATMENT OF HETEROGENEITY

In Section 2.4, it has been shown that:

$$\ln(C_{Ht}) = \ln(C_{Ho}) + \mu + N(0,\sigma) \quad \textbf{(3.1)}$$

or, alternatively:

$$C_{Ht} = C_{Ho}\, C_F \exp(N(0,\sigma)) \quad \textbf{(3.2)}$$

where:

C_F = $\exp(\mu)$

μ = $\mu\left(\frac{x}{X_W},\frac{y}{X_W},\frac{\alpha_T}{X_W},Var(ln\ K)\right)$

= Mean of natural logarithmic concentration ratio

σ = $\sigma\left(\frac{x}{X_W},\frac{y}{X_W},\frac{\alpha_T}{X_W},Var(ln\ K)\right)$

= Standard deviation of natural logarithmic concentration ratio

Note that μ and σ may be obtained by multiplying 2.303 to the means and standard deviations of $\log_{10}(C_{ht}/C_{ho})$.

In order to avoid introducing bias into the corrected concentration due to the inclusion of the stochastic component, the following constraint is applied:

$$E(C_{Ht}) = E(C_{Ho}C_F) \quad \textbf{(3.3)}$$

which leads to the following bias correction in Equation (3.2):

$$C_{Ht} = C_{Ho}\, C_F \frac{\exp(N(0,\sigma))}{\exp(0.5\sigma^2)} \quad \textbf{(3.4)}$$

draft

3.2 INCORPORATION OF HETEROGENEITY EFFECTS IN EPACMTP SIMULATIONS

For the i-th realization in EPACMTP, with i = 1, 2, …, N,

- Generate a well location, $X_{WELL,\ i}$, $Y_{WELL,\ i}$, from a given CDF for well distance, and normalize the well location using the site-based source dimension, X_{wi}, thus:

$$x' = \frac{X_{Well,\ i}}{X_{Wi}} \qquad y' = \frac{Y_{Well,\ i}}{X_{Wi}} \qquad \textbf{(3.5)}$$

- Generate a longitudinal dispersivity, α_L, from a given CDF for α_L, and correct for the well distance. Generate a corresponding lateral dispersivity, α_T, from a predetermined dispersivity ratio α_L / α_T

- Generate a value of *Var(ln K)* from a given CDF for *Var(ln K)*.

- Use the normalized well location (Equation (3.4)), normalized lateral dispersivity, and *Var(ln K)*, in conjunction with Equation (3.3) to determine mean of logarithmic concentration ratio, μ, and the associated standard deviation, σ, by linear interpolation between data points in the grid system of values of dispersivity, and variance of *ln K*.

- Determine a correction factor *R* as:

$$R = \frac{\exp(\mu)\exp(N(0,\sigma))}{\exp(0.5\sigma^2)} \quad with \quad -3\sigma \le N(0,\sigma) \le 3\sigma; \quad \log_{10}(\exp(\mu)) \le 3 \qquad \textbf{(3.6)}$$

- Determine concentration due to the presence of heterogeneity using the relationship below:

$$C_{Ht} = C_{Ho} \cdot R \le C_o \qquad \textbf{(3.7)}$$

US EPA ARCHIVE DOCUMENT

where

C_o = concentration at the source

3.3 RESULTS OF EPACMTP SIMULATIONS WITH HETEROGENEITY

A number of EPACMTP simulations, each with 10,000 realizations, were carried out to assess the potential effects due to the presence of heterogeneity. Relevant site parameters (waste management unit dimension, and lateral dispersivity) were obtained from the Subtitle D industrial landfill data base used for HWIR 1995 groundwater pathway analysis (U.S.EPA, 1995, 1997). In each realization, model prediction correction associated with heterogeneity was introduced through the procedure outlined in Section 3.2.

There are two cases of potential interest:

- Constant variance of *ln K*
- Probabilistic variance of *ln K*

Results from the above two cases are presented in the following subsections.

3.3.1 Case 1 - Constant Variance of ln *K*

Results from 6 sets of EPACMTP simulations with *Var*(ln *K*) varying from 0 to 6.1 are shown in Figure 3.1. Concentrations corresponding to selected percentiles are shown in Table 3.1. In the figure and the table, one can readily see that for a given percentile, concentration at receptor well increases with the increase in *Var* (ln *K*). In the table, a general trend may be observed. For a given percentile, the concentrations generated by the heterogeneous model tend to be greater than those from the homogeneous model. The difference between the two concentrations is proportional to the value of *Var* (ln *K*).

3.3.2 Case 2 - Probabilistic Variance of *ln* K - Global Data

A literature search was conducted by Dynamac Corporation (Dynamac Corp., 1998) to determine the distribution of Var(*ln K*) nationwide. Based on published information from 98 measurement sites in 41 locations nationwide, a CDF for *Var*(ln *K*) is presented in Table 3.2. It should be noted that the CDF consists of data obtained from multiple test types, often at the same sites. Equal weights were given to all the *Var*(ln *K*) values obtained from different test types. At a site, *Var*(ln *K*) values obtained from different test types were treated as unique data points.

In Section 2, the maximum variance of ln *K* is approximately 6.1 which is greater than *Var*(ln *K*) of 94 percent of the measurement sites (92 sites of the total of 97 sites). In the CDF in Table 3.2,

US EPA ARCHIVE DOCUMENT

the maximum value of *Var*(ln *K*) is 13.3. For sites in which Var(*ln K*) is greater than 6.1, the value of Var(*ln K*) was set to 6.1 in the analysis.

Results are shown in Figure 3.2. Concentrations corresponding to selected percentiles are shown in Table 3.3. As shown in the table, the post- 90th percentile values of the heterogeneity-influenced concentrations are from 35 to 48 percent greater than the corresponding homogeneity-based concentrations.

3.3.3 Case 3 - Probabilistic Variance of *ln K* - Pump Test Data

Var(*ln K*) values based on pump test data or combined pump test and slug test data were extracted from the data base used to construct the CDF in Case 2. A CDF based on pump test data and combined pump test and slug test data is presented in Table 3.4. A total of 10 data sets were available. Details of these tests are provided in Appendix B of this report. This CDF is considered more realistic than the CDF based on global data used in Section 3.3.2.

The maximum value of *Var*(ln *K*) is 3.34 which is within the range of *Var*(ln *K*) values used in Section 2 to develop correction factors for heterogeneity effects.

Results are shown in Figure 3.3. Concentrations corresponding to selected percentiles are shown in Table 3.3. As shown in the table, the post- 90th percentile values of the heterogeneity-influenced concentrations are from 9 to 25 percent greater than the corresponding homogeneity-based concentrations.

US EPA ARCHIVE DOCUMENT

draft

US EPA ARCHIVE DOCUMENT

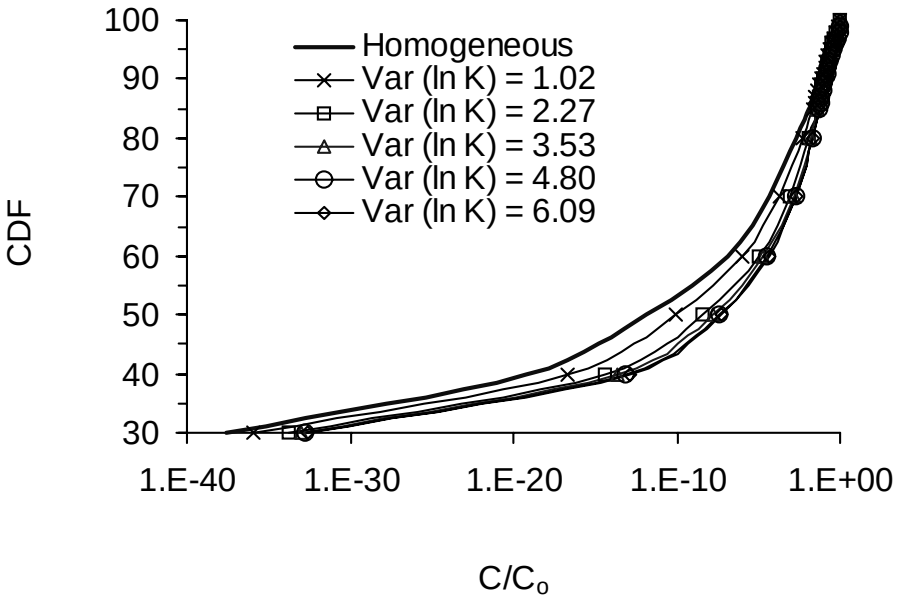

3.1 (a)

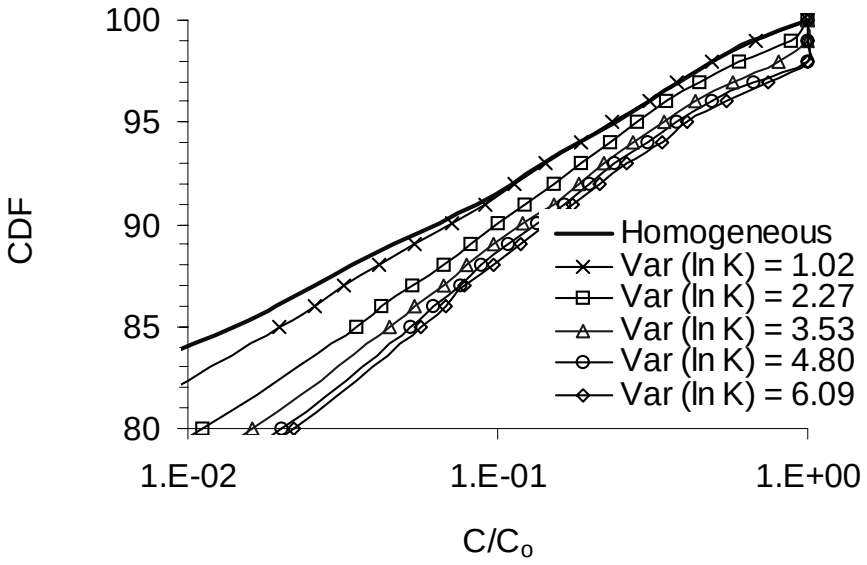

3.1 (b)

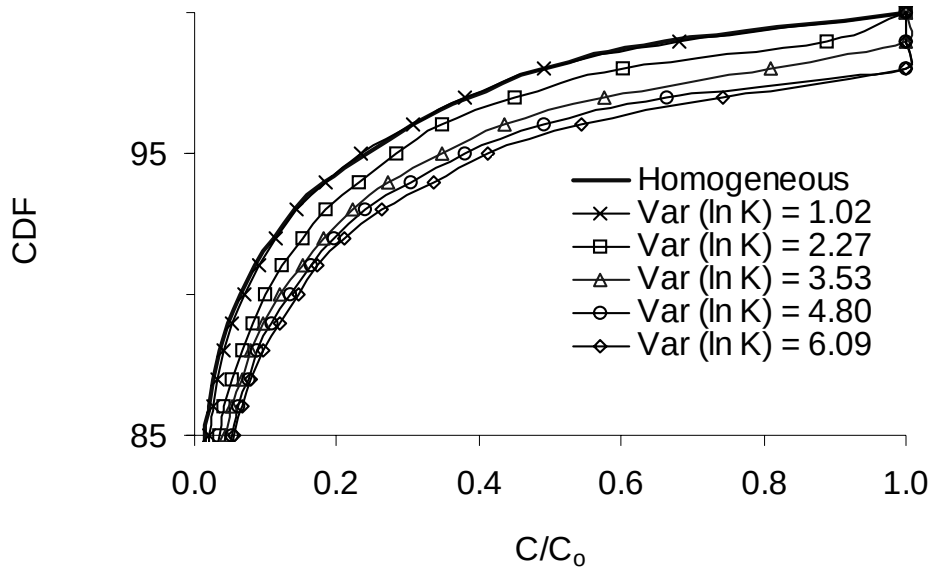

3.1 (c)

Figure 3.1 Comparison of CDF with and without Heterogeneity for the Case with Constant Variance of *ln K*: (a) Logarithmic Scale, (b) Logarithmic Scale for Limited Range, and (c)Arithmetic Scale.

US EPA ARCHIVE DOCUMENT

Table 3.1 Normalized Receptor Well Concentrations for Selected Percentiles: Constant Variance of Ln (K)

Percentile	C/C_o					
	Homogeneous Case	Constant Variance of *ln K*: (Variance of *ln K*)				
		(1.02)	(2.27)	(3.53)	(4.80)	(6.09)
10	0.00E+00	0.00E+00	0.00E+00	0.00E+00	0.00E+00	0.00E+00
20	0.00E+00	0.00E+00	0.00E+00	0.00E+00	0.00E+00	0.00E+00
30	2.99E-38	1.20E-36	1.56E-34	9.18E-34	2.07E-33	2.64E-33
40	5.20E-20	1.92E-17	4.12E-15	2.56E-14	6.61E-14	1.22E-13
50	1.57E-12	7.88E-11	4.15E-09	1.92E-08	4.20E-08	5.98E-08
60	1.22E-07	1.14E-06	9.50E-06	2.11E-05	3.29E-05	4.57E-05
70	4.89E-05	2.12E-04	8.38E-04	1.43E-03	1.85E-03	2.16E-03
80	2.32E-03	5.11E-03	1.11E-02	1.62E-02	2.00E-02	2.20E-02
85	1.41E-02	1.99E-02	3.51E-02	4.50E-02	5.24E-02	5.65E-02
86	1.91E-02	2.57E-02	4.18E-02	5.36E-02	6.20E-02	6.83E-02
87	2.55E-02	3.19E-02	5.28E-02	6.65E-02	7.54E-02	7.86E-02
88	3.42E-02	4.12E-02	6.68E-02	7.94E-02	8.85E-02	9.66E-02
89	4.64E-02	5.38E-02	8.16E-02	9.73E-02	1.09E-01	1.19E-01
90	6.46E-02	7.15E-02	1.00E-01	1.20E-01	1.33E-01	1.45E-01
91	8.54E-02	9.06E-02	1.23E-01	1.51E-01	1.64E-01	1.74E-01
92	1.11E-01	1.14E-01	1.51E-01	1.83E-01	1.97E-01	2.12E-01
93	1.42E-01	1.42E-01	1.85E-01	2.21E-01	2.39E-01	2.63E-01
94	1.82E-01	1.85E-01	2.30E-01	2.73E-01	3.04E-01	3.37E-01
95	2.42E-01	2.35E-01	2.84E-01	3.47E-01	3.79E-01	4.11E-01
96	3.08E-01	3.07E-01	3.47E-01	4.37E-01	4.91E-01	5.44E-01
97	3.85E-01	3.80E-01	4.50E-01	5.77E-01	6.64E-01	7.44E-01
98	4.91E-01	4.92E-01	6.02E-01	8.10E-01	1.00E+00	1.00E+00
99	6.62E-01	6.81E-01	8.89E-01	1.00E+00	1.00E+00	1.00E+00
100	1.00E+00	1.00E+00	1.00E+00	1.00E+00	1.00E+00	1.00E+00

US EPA ARCHIVE DOCUMENT

Table 3.2 Distribution of Variances of *log K* and *ln K* - Global Data.

Cumulative Probability	Var(*Log K*)	Var(*ln K*)
0.0	0.0	0.0
0.38	0.1	0.53
0.40	0.2	1.06
0.49	0.3	1.59
0.58	0.4	2.12
0.62	0.5	2.65
0.70	0.6	3.18
0.75	0.7	3.71
0.80	0.8	4.24
0.85	0.9	4.77
0.90	1.0	5.30
0.94	1.1	5.83
0.97	1.5	7.96
0.99	2.0	10.6
1.00	2.5	13.3

US EPA ARCHIVE DOCUMENT

draft

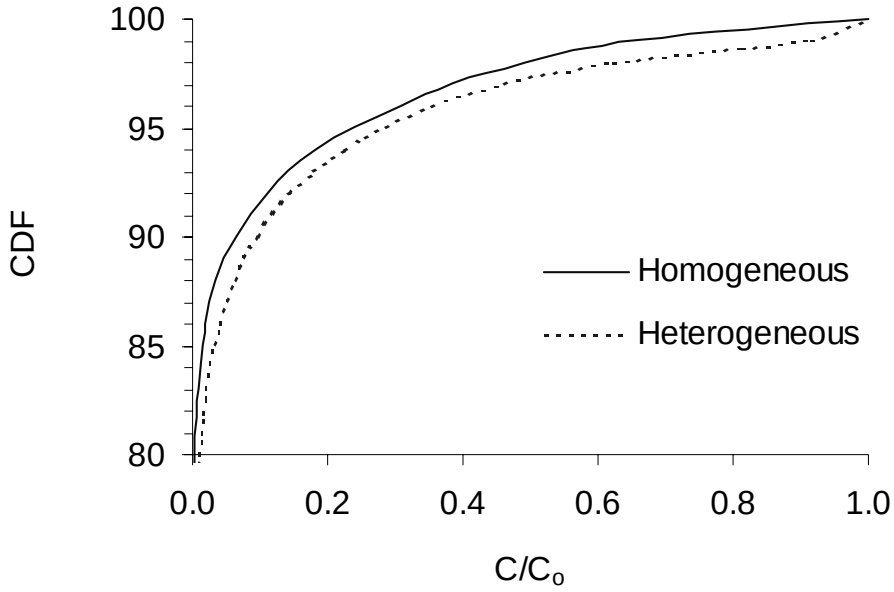

Figure 3.2 Comparison of CDF with and without Heterogeneity for the Case with Probabilistic Variance of *ln K* - Global Data

US EPA ARCHIVE DOCUMENT

Table 3.3 Normalized Receptor Well Concentrations for Selected Percentiles: Global Ln (K) Data and Pump-Test Ln (K) Data

Percentile	C/C_o		
	Homogeneous Case	Probabilistic Variance of *ln K*	
		Global data(1)	Pump test data(2)
10	0.00E+00	0.00E+00	0.00E+00
20	0.00E+00	0.00E+00	0.00E+00
30	2.99E-38	6.99E-35	8.07E-36
40	5.20E-20	5.05E-16	9.72E-17
50	1.57E-12	1.57E-09	3.39E-10
60	1.22E-07	5.42E-06	2.46E-06
70	4.89E-05	5.65E-04	3.52E-04
80	2.32E-03	9.31E-03	6.56E-03
85	1.41E-02	3.03E-02	2.52E-02
86	1.91E-02	3.85E-02	3.08E-02
87	2.55E-02	4.78E-02	3.89E-02
88	3.42E-02	6.10E-02	4.90E-02
89	4.64E-02	7.52E-02	6.37E-02
90	6.46E-02	9.55E-02	8.08E-02
91	8.54E-02	1.18E-01	1.01E-01
92	1.11E-01	1.44E-01	1.27E-01
93	1.42E-01	1.82E-01	1.57E-01
94	1.82E-01	2.28E-01	1.99E-01
95	2.42E-01	2.87E-01	2.55E-01
96	3.08E-01	3.54E-01	3.26E-01
97	3.85E-01	4.63E-01	4.05E-01
98	4.91E-01	6.20E-01	5.45E-01
99	6.62E-01	9.15E-01	7.26E-01
100	1.00E+00	1.00E+00	1.00E+00

Notes: (1) Variance of *ln* K derived from all types of test in the data base (Dynamac Corp., 1998).

(2) Variance of *ln* K derived from pump test and slug test data in the data base (Dynamac Corp., 1998). See also Appendix B.

US EPA ARCHIVE DOCUMENT

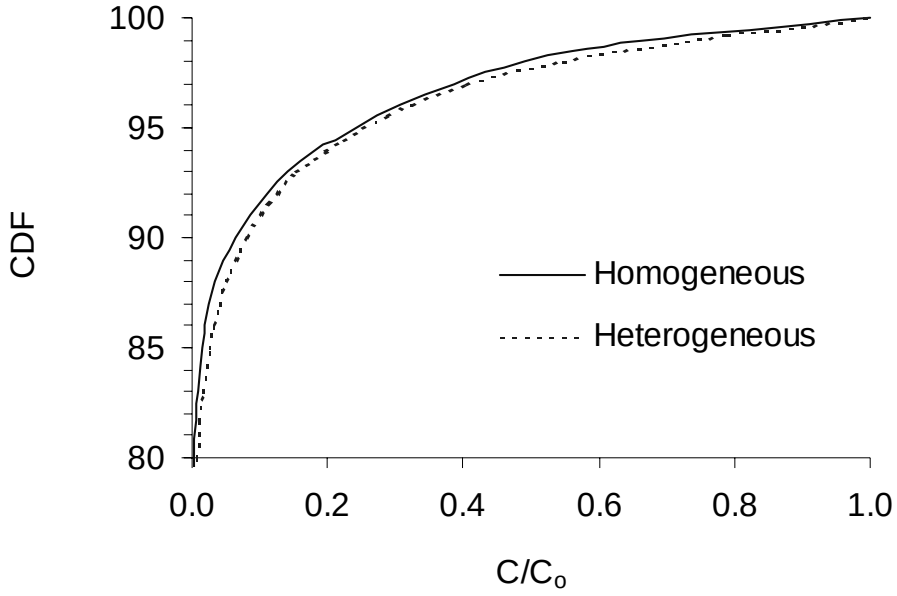

Figure 3.3 Comparison of CDF with and without Heterogeneity for the Case with Probabilistic Variance of *ln K* - Pump Test Data

US EPA ARCHIVE DOCUMENT

Table 3.4 Distribution of Variances of *log K* and *ln K* - Pump Test Data.

Cumulative Probability	Var(*Log K*)	Var(*ln K*)
0.0	0.00	0.0
0.20	0.01	0.05
0.30	0.03	0.16
0.40	0.06	0.32
0.50	0.07	0.37
0.60	0.08	0.42
0.70	0.34	1.80
0.80	0.40	2.12
0.90	0.55	2.92
1.00	0.63	3.34

US EPA ARCHIVE DOCUMENT

draft

US EPA ARCHIVE DOCUMENT

4.0 SUMMARY

A methodology to incorporate the effects due to heterogeneity into the Monte-Carlo analysis of groundwater pathway risk assessment has been developed. A numerical model in conjunction with the Fourier Spectral technique was employed to generate a set of realizations of spatially heterogeneous hydraulic conductivity and porosity, and to perform flow and transport simulations for the generated realizations. The results were compiled to determine spatial distributions of means and standard deviations of correction for predicted concentrations.

Results from a set of runs with constant variance of natural logarithm of hydraulic conductivity indicated that the concentrations generated by the heterogeneous model tend to be greater than those from the homogeneous model. The difference between the two concentrations is proportional to the value of variance of natural logarithm of hydraulic conductivity.

Results from a preliminary test with a nationwide distribution of intra-site variance of natural logarithm of hydraulic conductivity indicated that for the same percentile receptor well concentrations subjected to heterogeneity are consistently greater than the corresponding concentrations due to homogeneous settings. Using a CDF of variance of ln K based on nation wide pump test data (or combined pump test and slug test data), the post-90^{th} percentile concentrations with heterogeneity effects are from 9 to 25 percent greater than the corresponding concentrations without heterogeneity effects.

draft

5.0 REFERENCES

Bear, J. Hydraulics of Groundwater McGraw Hill, New York, 1979.

Davis, S. N. Porosity and Permeability of natural materials. In: Flow Through Porous Media, R. J. M. de Wiest, Editor, Academic Press, NY, 1969.

Dynamac Corporation. Characterization of Hydraulic Properties of Potentially Fractured Industrial D Landfill Sites and A Study of Heterogeneity Effects on Fate and Transport in Groundwater, 1998.

Gelhar, L. W. Stochastic Subsurface Hydrology. Prentice-Hall, 1993.

HydroGeoLogic, Inc. MODFLOW-SURFACT (Version 1.2). The HydroGeoLogic Enhanced Version of the U.S. Geological Modular Flow Model, Code Documentation Report, 1996.

McDonald, M.G., and Harbaugh, A.W. A Modular Three-Dimensional Finite-Difference Ground-Water Flow Model: U.S. Geological Survey Techniques of Water Resources Investigations Book 6, Chapter A1, 1988.

Minitab, Inc. MINITAB (Version 12.1), 1998.

Robin, M.J.L., Gutjahr, A.L., Sudicky, E.A., and Wilson, J.L. Cross-Correlated Random Field Generation with the Direct Fourier Transform Method, Water Resources Research, 29(7), 2385-2397, 1993.

Statsoft, Inc. STATISTICA (Version 4.0), 1993.

U. S. EPA. Users Manual for EPA's Composite Model for Landfills (EPACML). U. S. EPA, Office of Solid Waste, Washington, D.C. 20460, 1990.

U. S. EPA. Hazardous Waste Identification Rule: Background Document for Groundwater Pathways Results. U. S. EPA, Office of Solid Waste, Washington, D.C. 20460, 1995.

U.S. EPA. EPA's Composite Model for Leachate Migration with Transformation Products (EPACMTP). Background Document, Office of Solid Waste, Washington, D.C., 20460, 1996a.

U. S. EPA. EPA's Composite Model for Leachate Migration with Transformation Products (EPACMTP). Background Document for Finite Source Methodology. U.S. EPA, Office of Solid Waste, Washington, D.C., 20460, 1996b.

US EPA ARCHIVE DOCUMENT

draft

U. S. EPA. EPA's Composite Model for Leachate Migration with Transformation Products (EPACMTP). Background document for Metals: Methodology. U.S. EPA, Office of Solid Waste, Washington, D.C., 20460, 1996c.

U.S. EPA. EPA's Composite Model for Leachate Migration with Transformation Products. User's Guide, Office of Solid Waste, Washington, D.C., 20460, 1997.

USEPA. The Vadose and Saturated Zone Modules Extracted from EPACMTP for HWIR99, U.S. EPA, Washington, D.C., 20460, 1999.

US EPA ARCHIVE DOCUMENT

draft

US EPA ARCHIVE DOCUMENT

APPENDIX A

FIGURES

draft

LIST OF FIGURES

US EPA ARCHIVE DOCUMENT

draft

US EPA ARCHIVE DOCUMENT

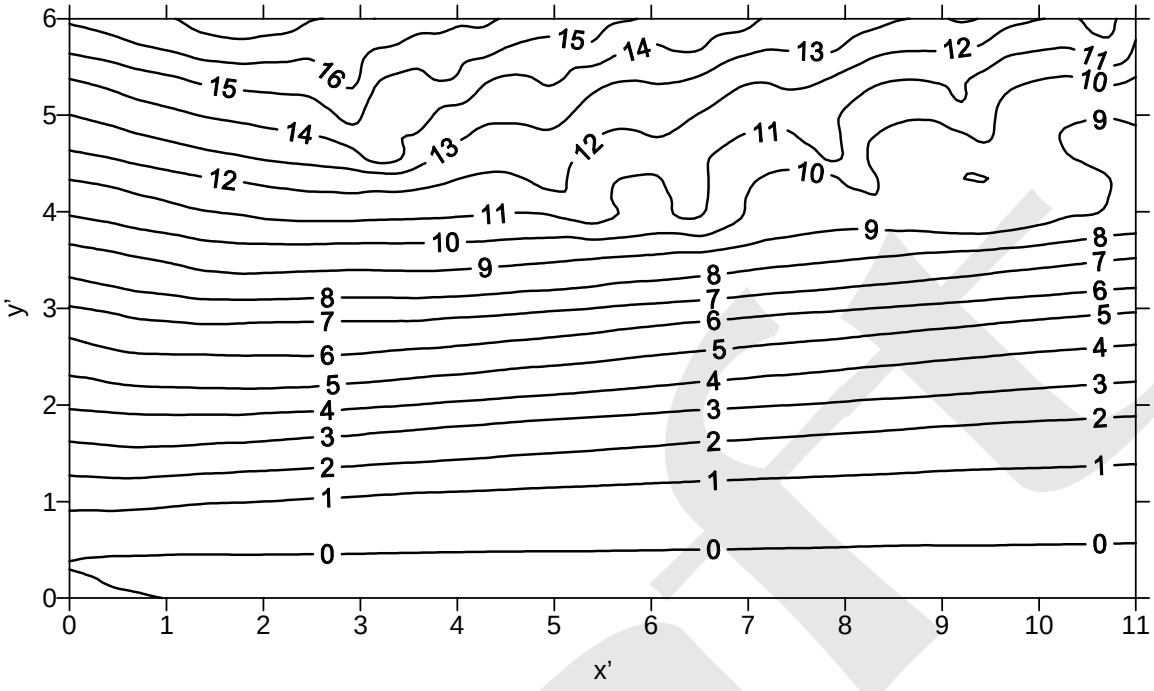

A1(a)

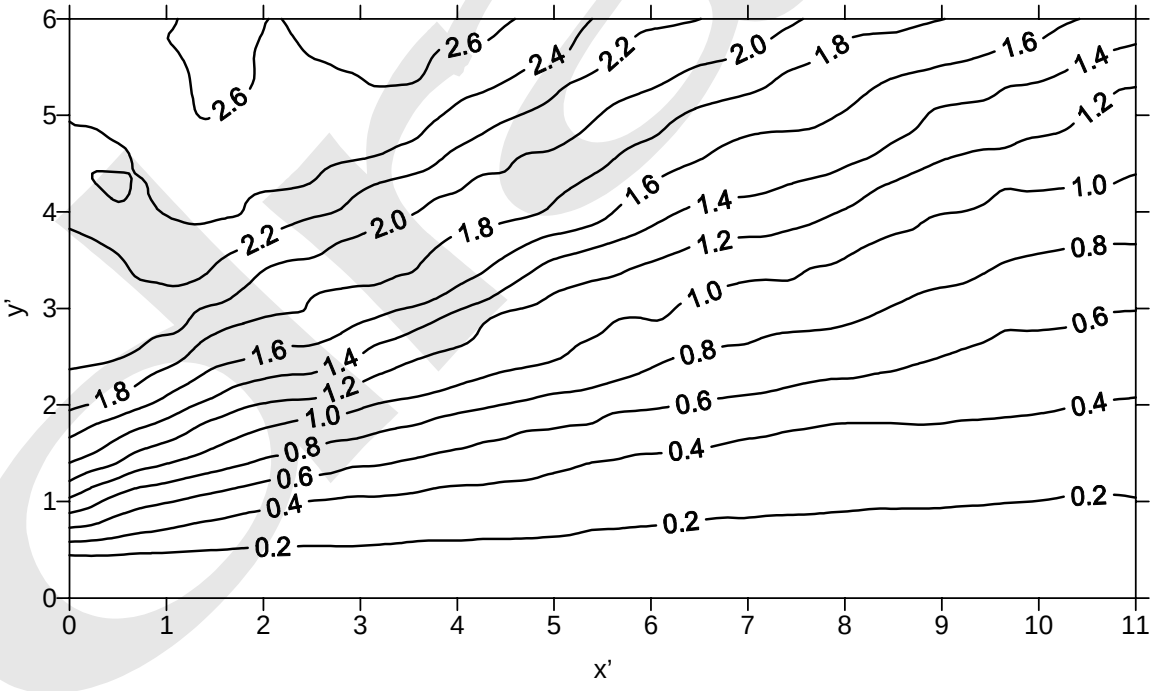

A1(b)

US EPA ARCHIVE DOCUMENT

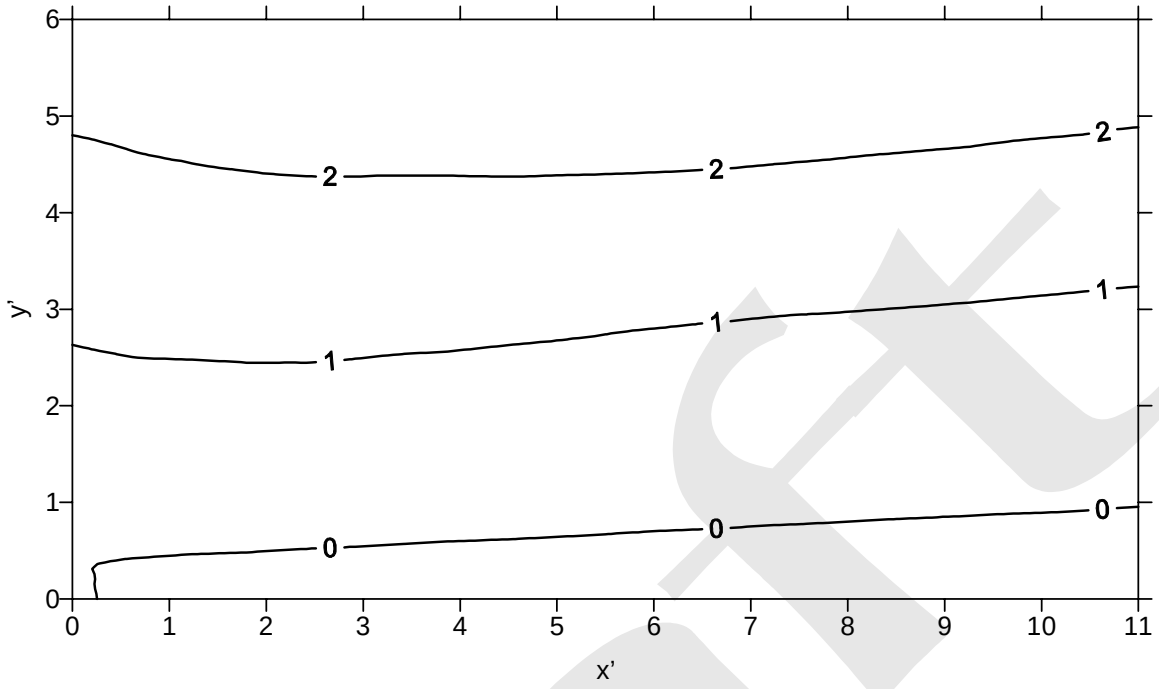

Figure A.2(a)

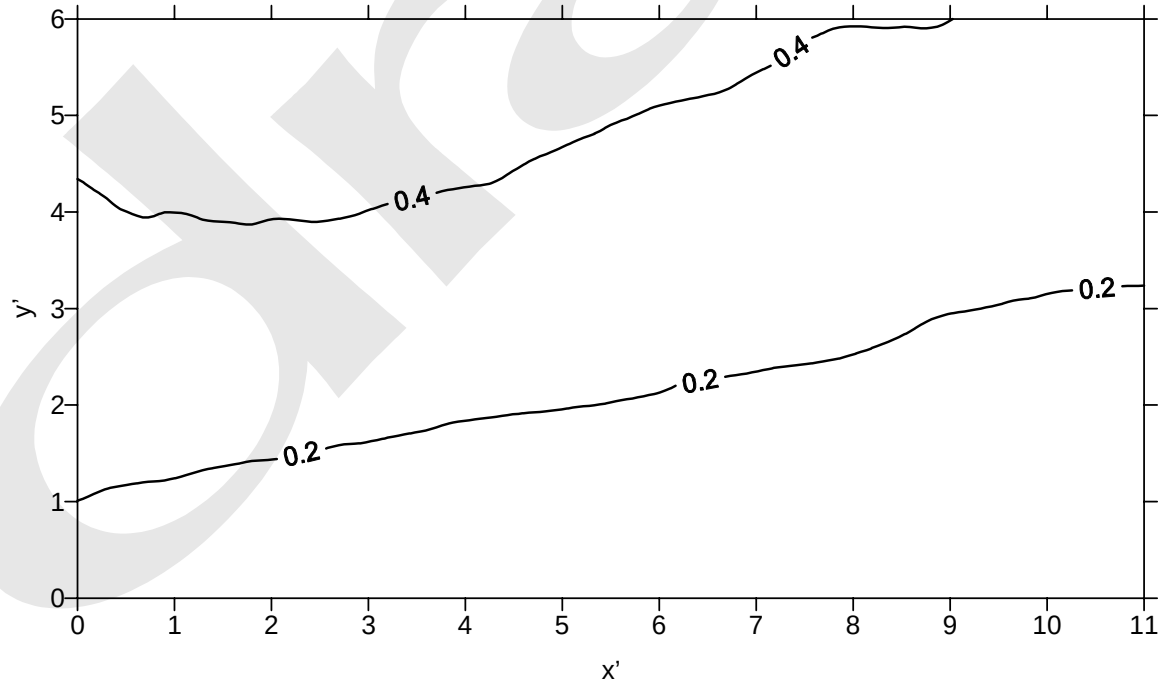

Figure A.2(b)

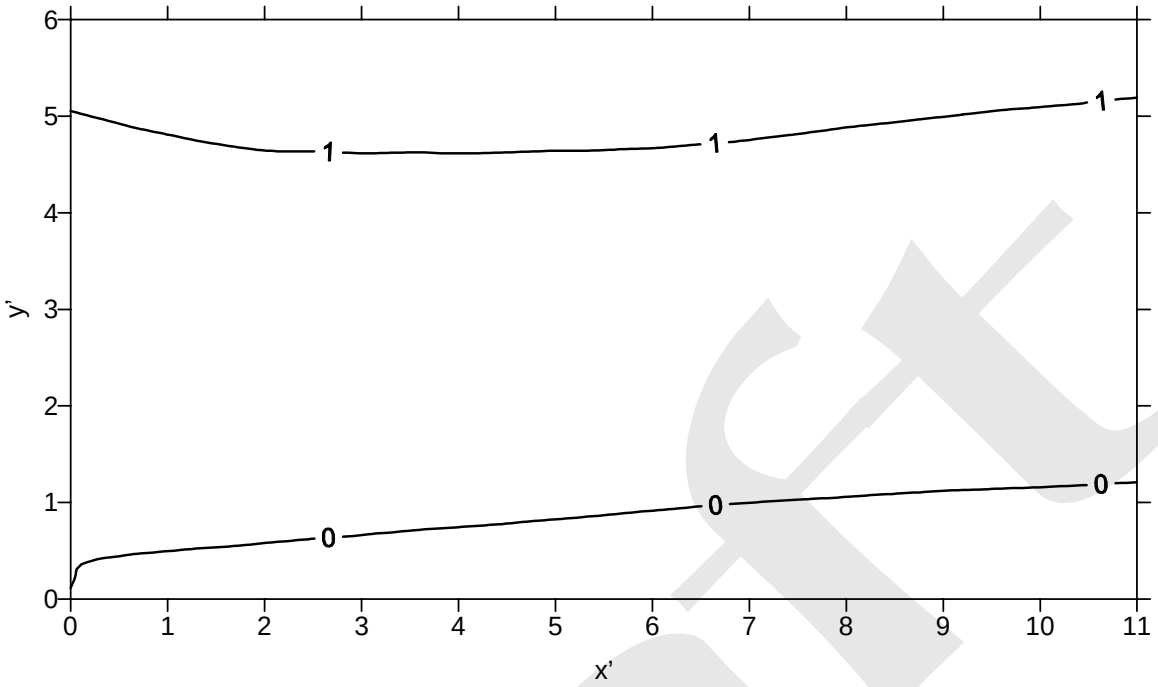

Figure A.3(a)

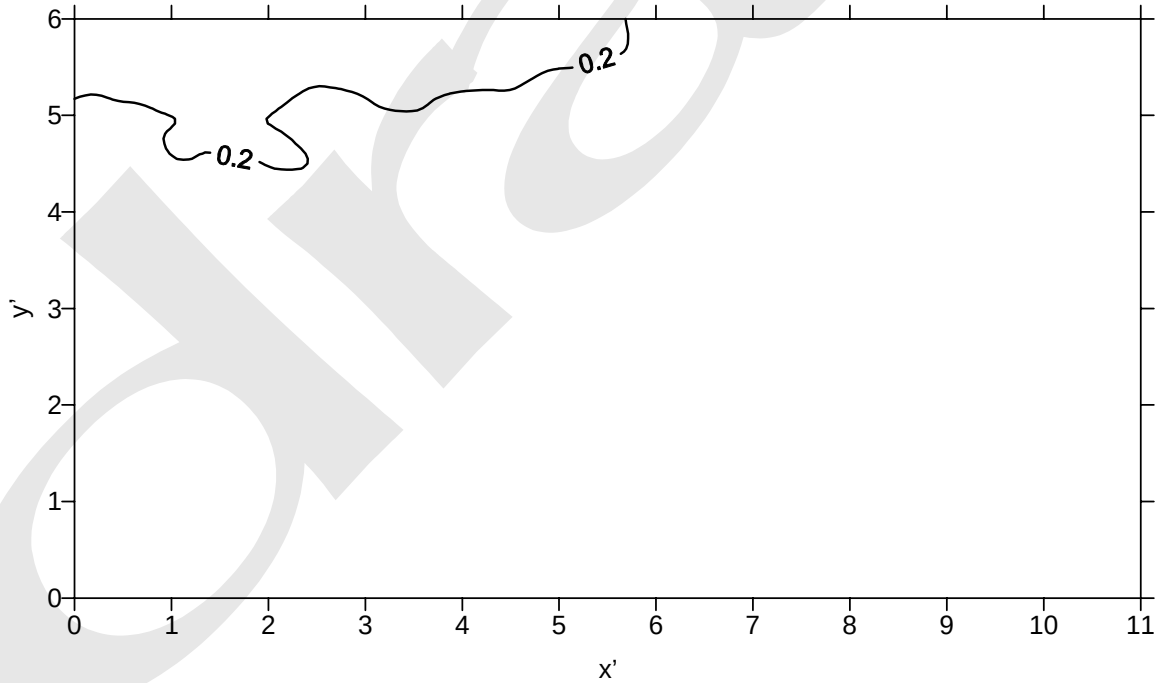

Figure A.3(b)

US EPA ARCHIVE DOCUMENT

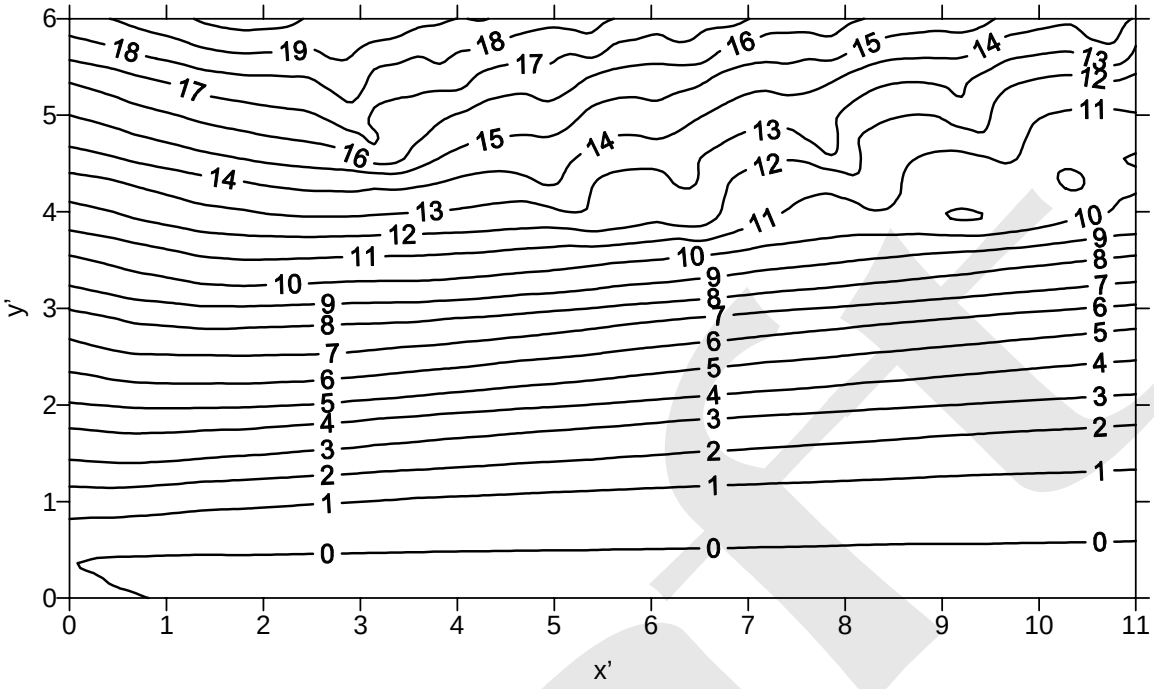

Figure A.4(a)

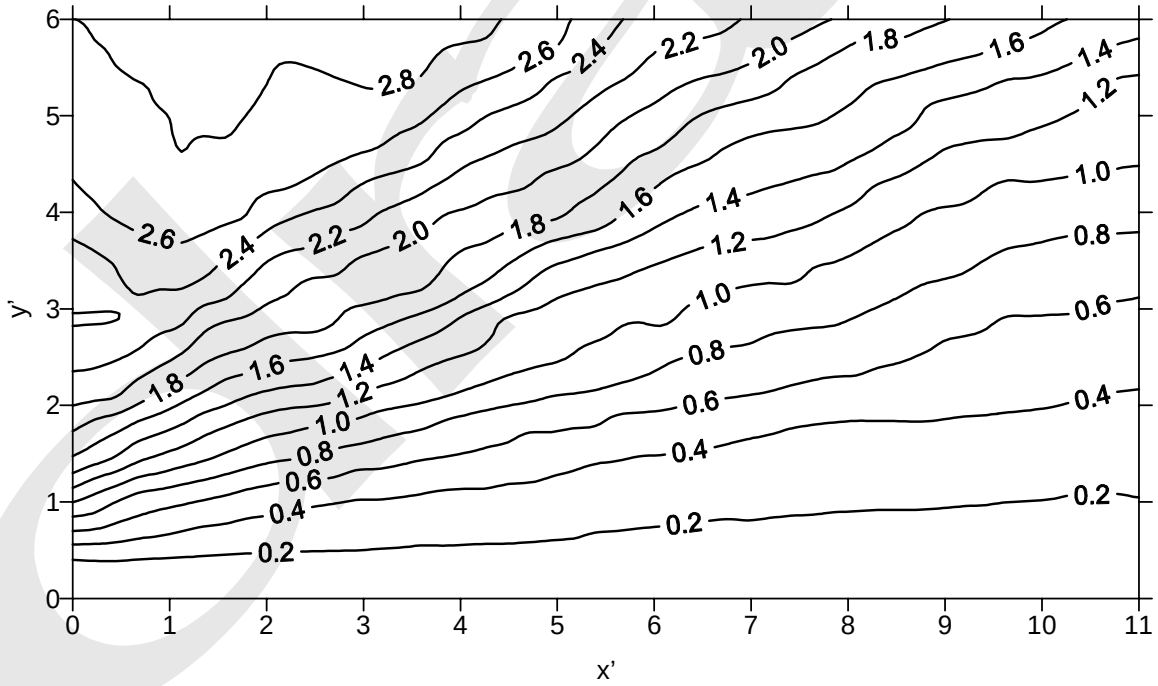

Figure A.4(b)

US EPA ARCHIVE DOCUMENT

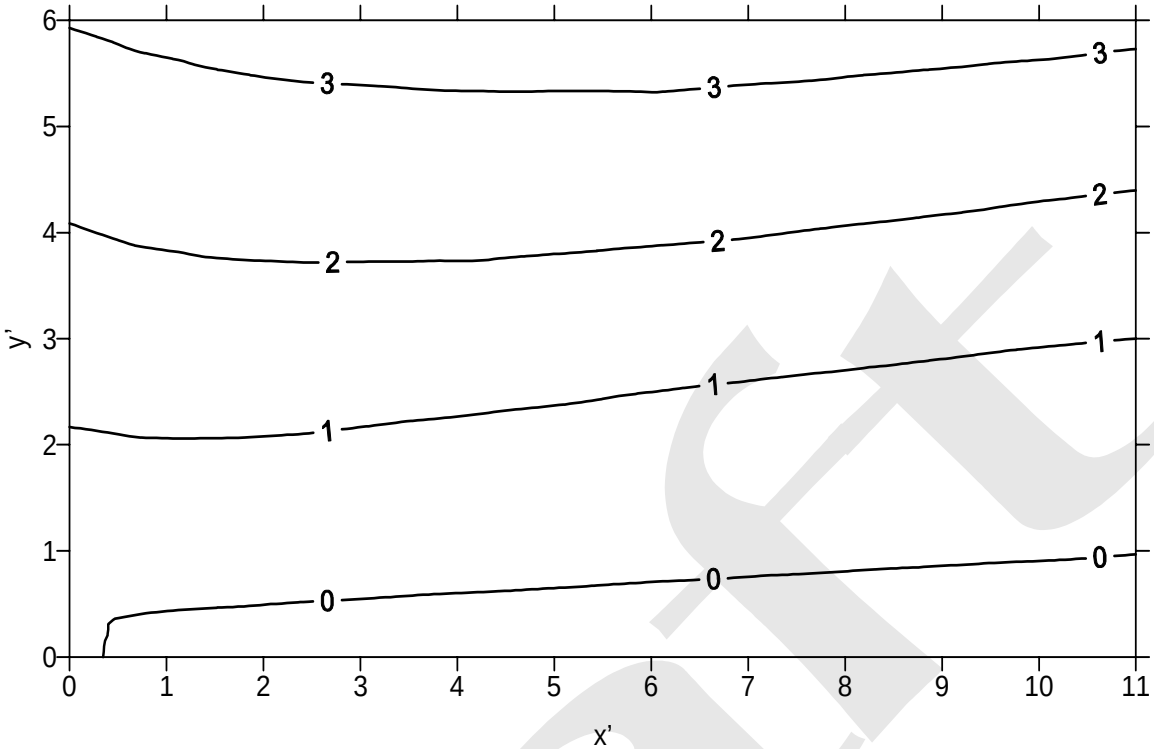

Figure A.5(a)

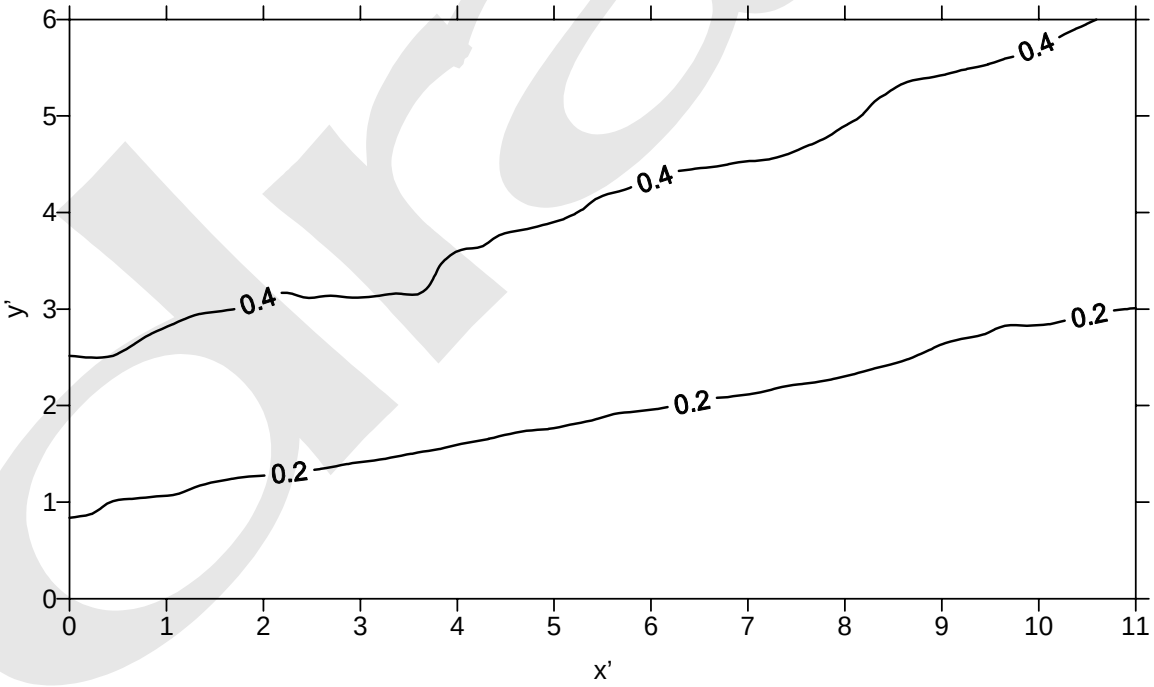

Figure A.5(b)

US EPA ARCHIVE DOCUMENT

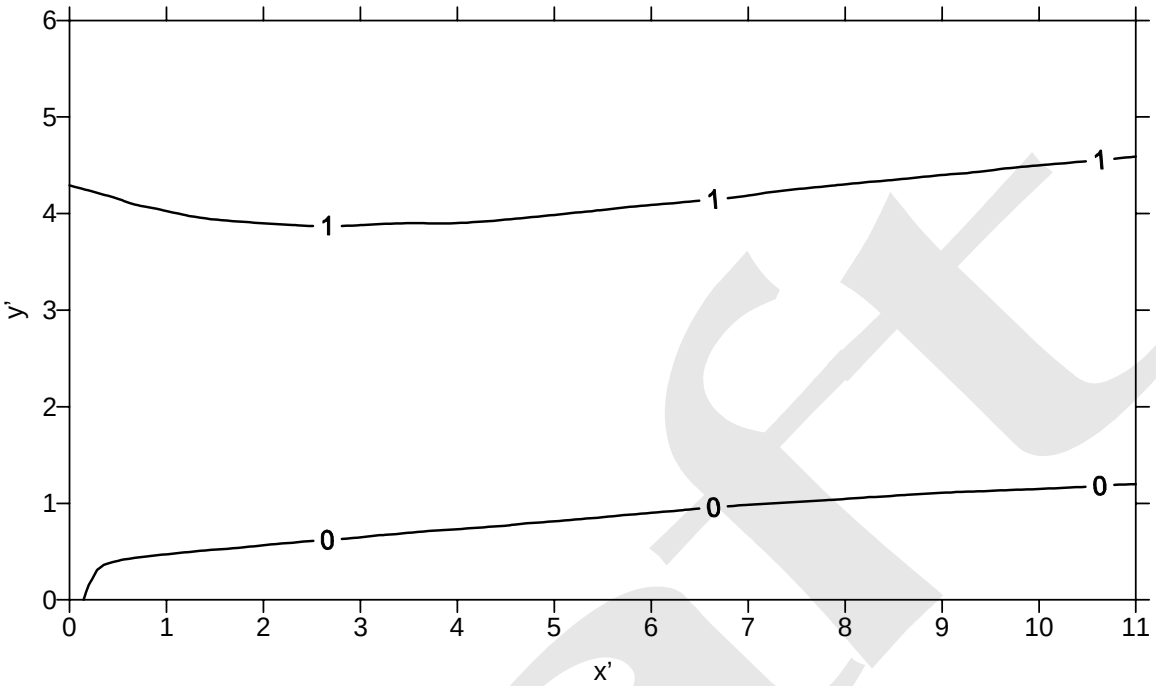

Figure A.6(a)

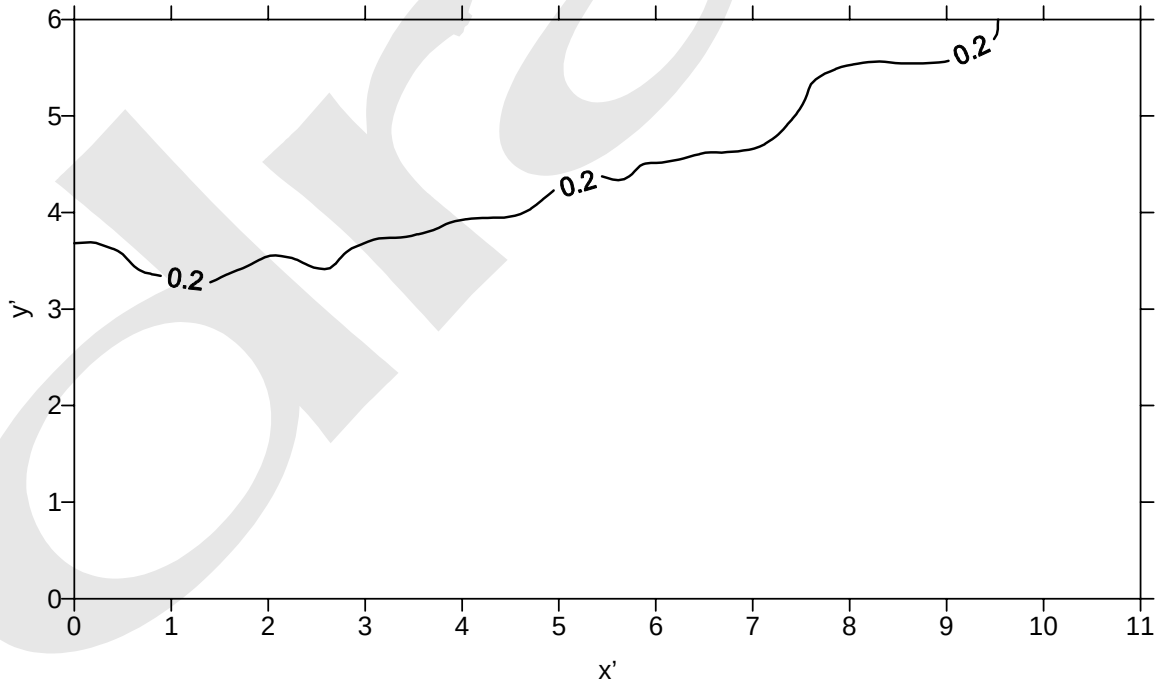

Figure A.6(b)

US EPA ARCHIVE DOCUMENT

draft

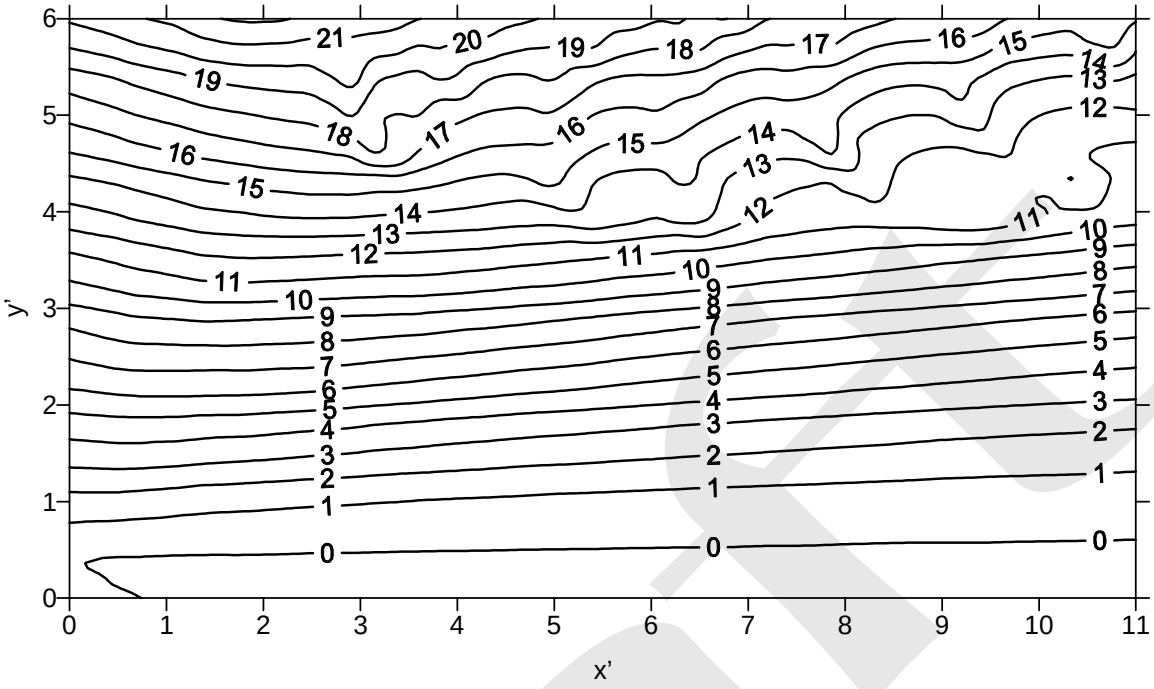

Figure A.7(a)

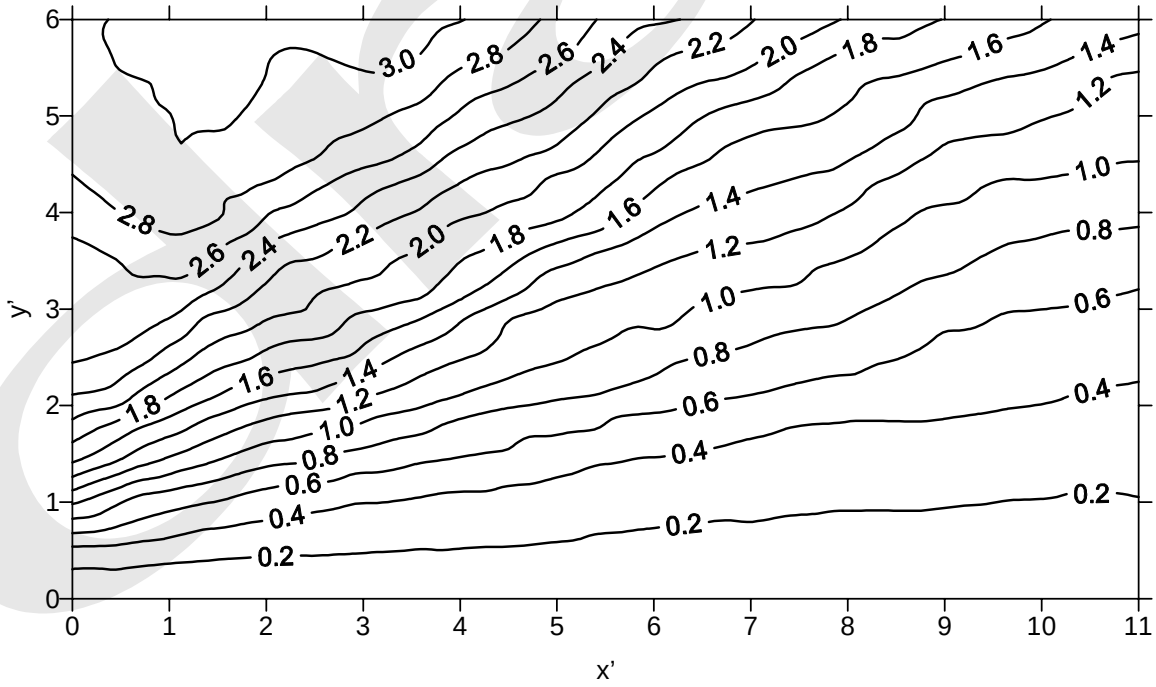

Figure A.7(b)

US EPA ARCHIVE DOCUMENT

US EPA ARCHIVE DOCUMENT

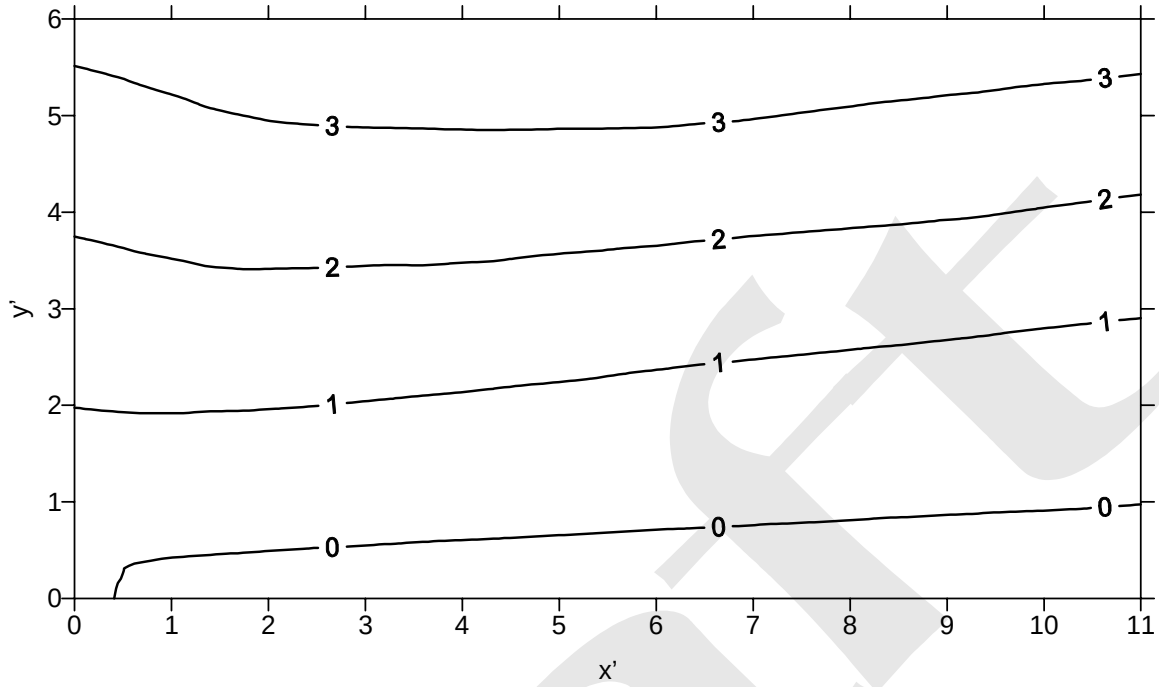

Figure A.8(a)

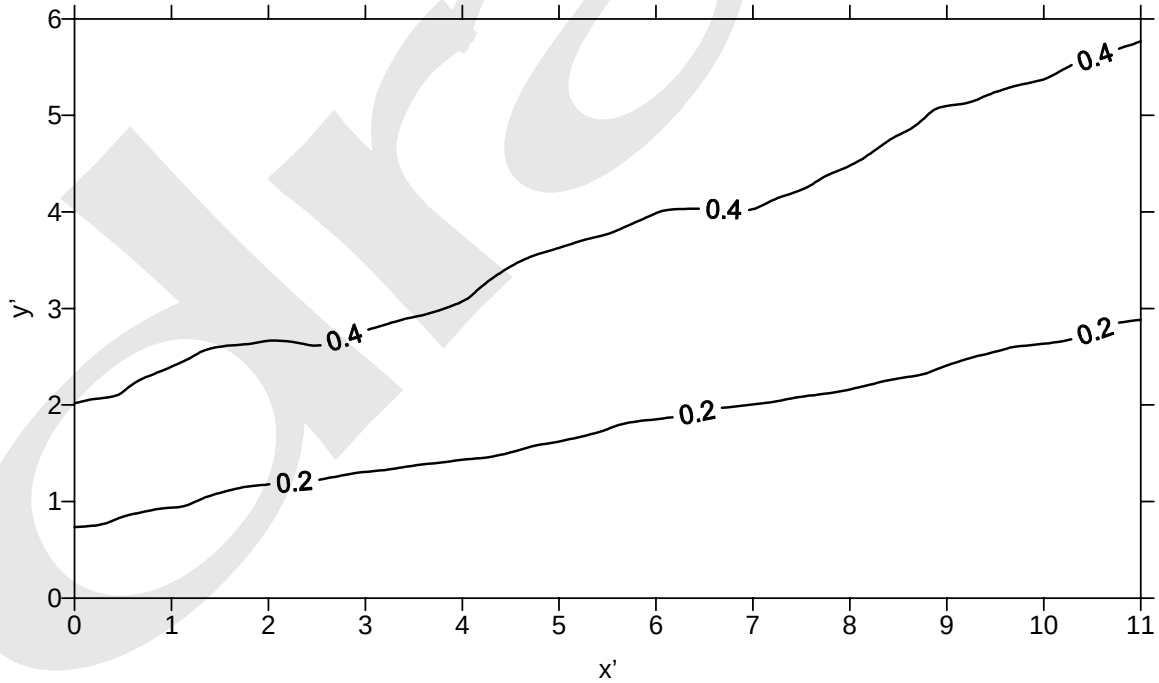

Figure A.8(b)

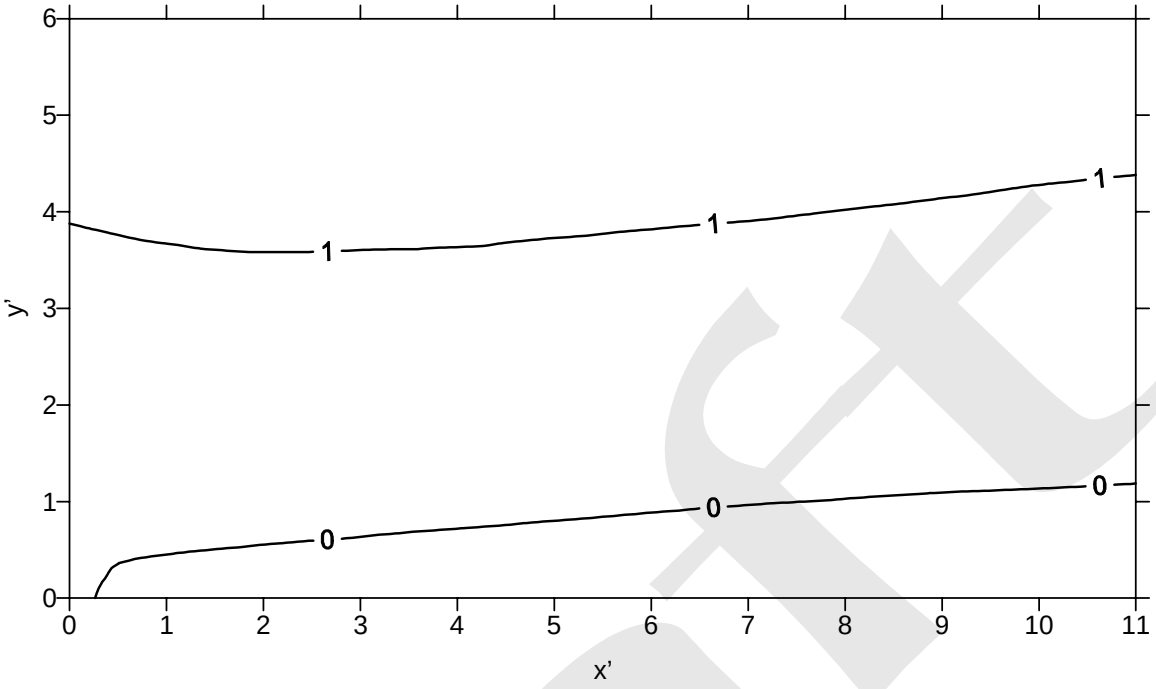

Figure A.9(a)

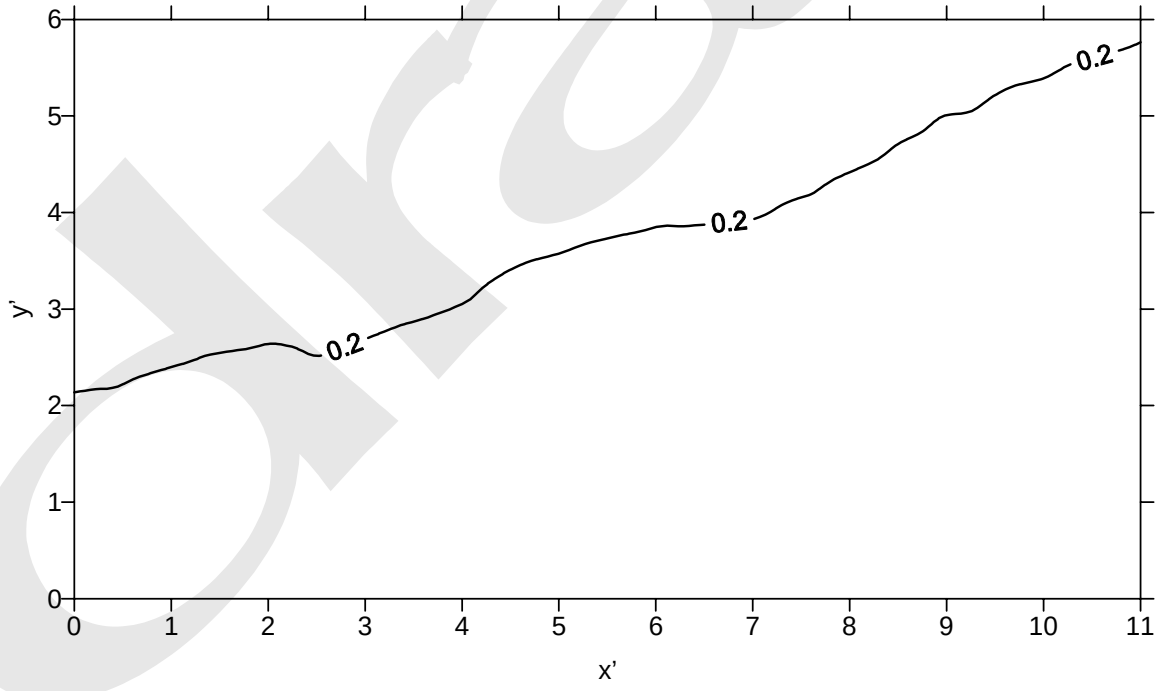

Figure A.9(b)

US EPA ARCHIVE DOCUMENT

draft

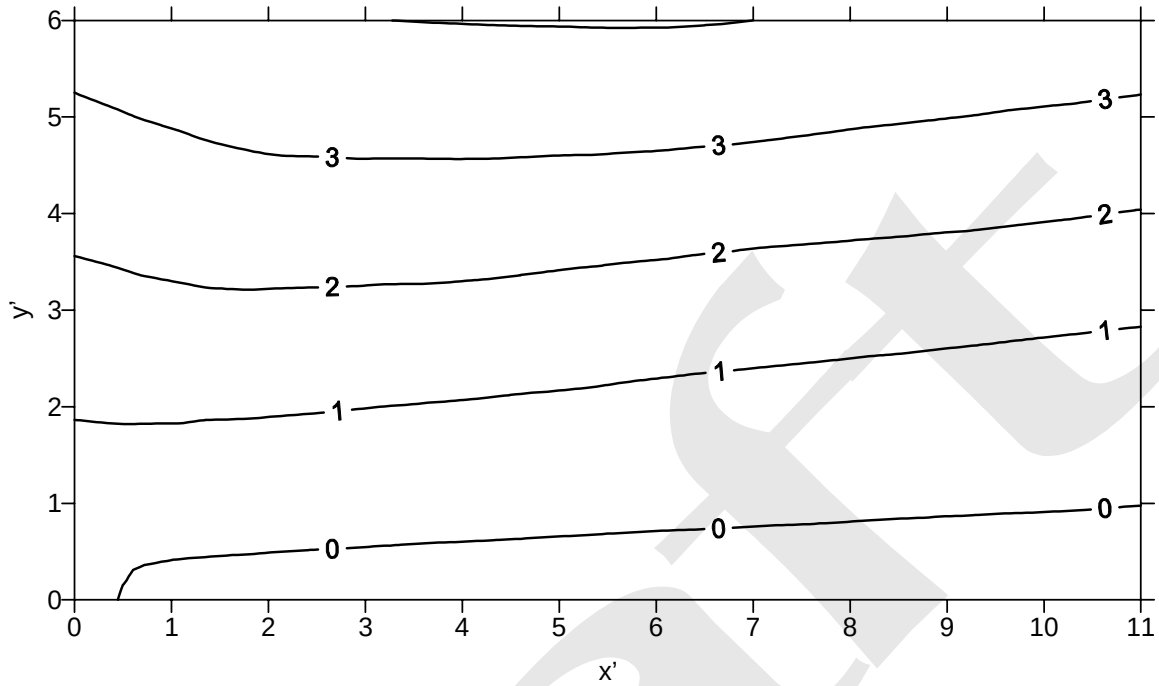

Figure A.10(a)

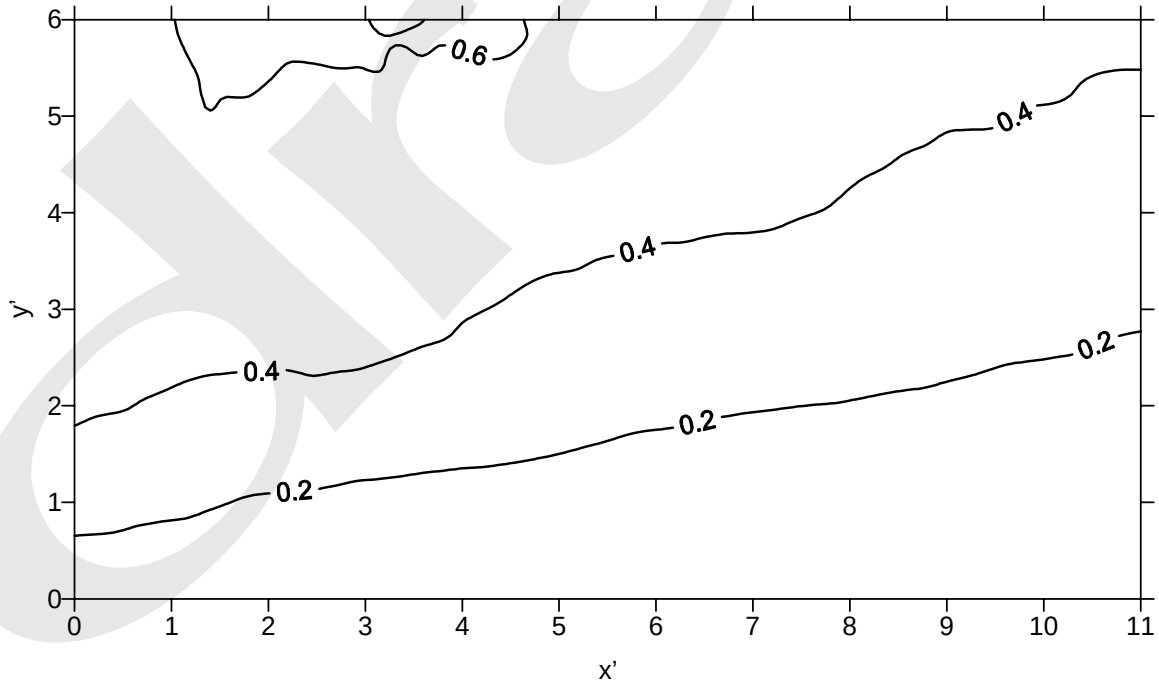

Figure A.10(b)

US EPA ARCHIVE DOCUMENT

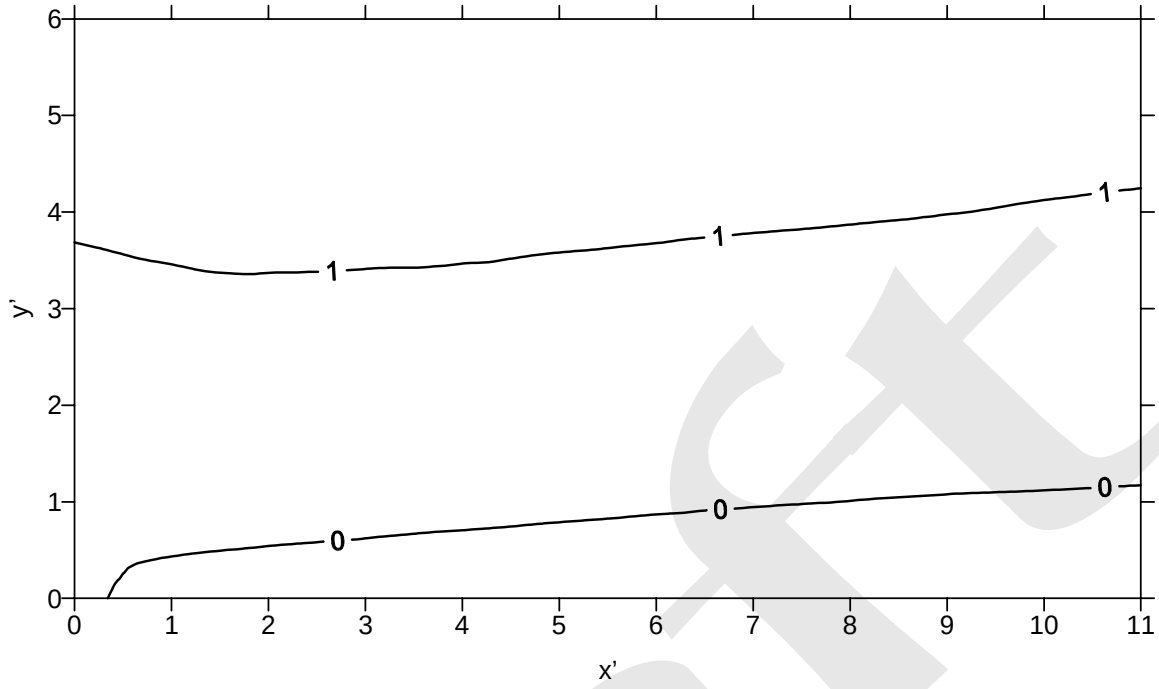

Figure A.11(a)

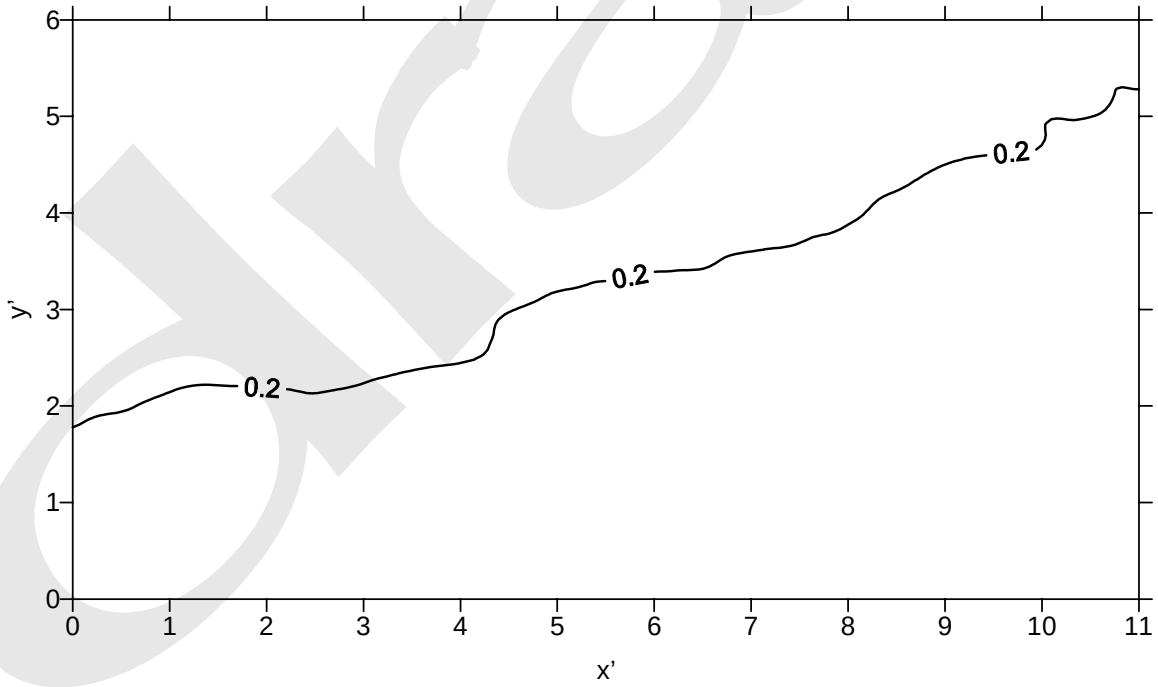

Figure A.11(b)

US EPA ARCHIVE DOCUMENT

draft

US EPA ARCHIVE DOCUMENT

APPENDIX B

AVAILABLE PUMP TEST DATA

draft

US EPA ARCHIVE DOCUMENT

Table B.1 Distribution of hydraulic conductivity values from selected papers.

Reference & Site Name	Aquifer Material	# of Test	Size of Test Zone	Estimation Method	Log of Hydraulic Conductivity or Permeability				Variance of Log (H/P)
					H/P[4]	Mean	Min	Max	
Way & McKee (1982), Sweetwater County, WY	fluvial sandstone & claystone	8	120 x 250 m 75 m thick	Pump test	H	-3.80	-3.97	-3.65	0.01
Norris (1983), Scioto River Valley, OH	sand & gravel outwash	13	7 miles long 40 - 65 ft thick	Pump test	H	-0.80	-1.00	-0.62	0.01
Urban & Gburek (1988), Willow Grove, PA	sandstone aquifer & shale	12 17 8 13 7	230x130 m 0.7-12 m thick	Grain size analysis pump test groundwater contour slug test recharge mound	H	-4.48 -3.15 -4.26 -3.39 -3.09	-4.56 -3.54 -4.57 -4.25 -3.34	-4.30 -2.53 -3.07 -2.53 -2.67	0.004 0.08 0.25 0.34 0.05
Taffet et al. (1989), San Joaquin County, CA	alluvial deposit	33	300 x 500 m 6 m thick	Pump & slug tests	H	-3.87	-5.52	-2.14	0.63
Capuano & Jan (1996), Galveston County, TX	Caly & silty-clay	16 16	2 wells 8 m thick	pump test (Theis curve) pump test (Time drawdoun)	H	-2.46 -2.50	-2.54 -2.62	-1.98 -1.87	0.02 0.03
Hill (1996), Yuma, AZ based on Hill (1993)	fluvial & deltaic sediments	30	20 x 20 miles 20-40 ft thick	pump test	H	-1.23	-1.75	-0.75	0.07
McCloskey & Finnemore (1996), San Jose, CA	alluvial basin sand & gravel	56	12 x 4 Km 100 m thick	11 pump tests 45 specific capacity tests	H	-1.74	-3.25	-0.62	0.55
Xiang (1996), Amarillo, TX	sand, gravel & clay	11	4 x 4 Km 160 m thick	pump test: Theis Cooper & Jacob Neuman	H	-2.04 -2.04 -2.40	-2.44 -2.44 -2.59	-1.61 -1.61 -2.22	0.06 0.06 0.02
Tompson et al. (1998) Livermore, CA	alluvial deposit	240	3.8 x 3.8 Km 100 m thick	pump, slug, and core tests	H	-2.93			0.34

Zhang & Brusseau (1998), Tucson, AZ	sand: lower 15 m thick sand: upper 20 m thick sand: upper 11 m thick	21 81 29	4 x 4 Km	pump test pump test Lab core test	H	-2.99 -1.81 -4.74	-3.75 -3.75 -6.30

Notes: (1) Kozeny-Carmen equation: $K = (\frac{\rho g}{\mu})[\frac{n^3}{(1-n^2)}](\frac{d^2}{180})$

(2) Hazen equation: K(m/day) = $A(d_{10})^2$, A=1.0, d_{10} = grain diameter (mm)

(3) Krumbein-Monk equation: $K = 760(GM_d)\{\theta^{-1.31\sigma}\}$, GM_d = Geometric mean diameter (mm), σ = standard deviation

(4) P = Permeability in cm^2; H = Hydraulic Conductivity in cm/sec.

US EPA ARCHIVE DOCUMENT

draft

REFERENCES

Capuano, R.M. & R.Z. In Situ hydraulic conductivity of clay and silty-clay fluvial-deltaic sediments, Texas Gulf Coast, Ground Water 34(3), p. 545-551, Jan 1996.

Hill, B.M. Use of numerical model for management of shallow ground-water levels in the Yuma, Arizona area, Ground Water, 34(3), p. 397-404, 1996.

McCloskey, T.F. and E.J. Finnemore. Estimating hydraulic conductivities in an alluvial basin from sediment facies methods, Ground Water, 34(6), p. 1024-1032, 1996.

Norris, S.E. Aquifer tests and well field performance, Scioto River Valley, Ohio: Part I, Ground Water, 21(3), p.287-292, 1983.

Taffet, M.J., J.A. Oberdorfer, W.A. McIlvride. Remedial investigation and feasibility study for the Lawrence Livermore National Laboratory Site 300 Pit 7 Complex, Lawrence Livermore National Lab, Livermore, CA, 1989.

Tompson, A.F.B., R.D. Falgout, S.G. Smith, W.J. Bosl, & F. Ashby. Analysis of subsurface contaminant migration and remediation using high performance computing, Water Resour. Res., Accepted for publication, 1998.

Urban, J.B., and W.J., Gburek. Determination of aquifer parameters at a ground-water recharge site, Ground Water 26(1), p. 39-53, 1988.

Way, S.C. & C.R. McKee, In-situ determination of three-dimensional aquifer permeabilities, Ground Water, 20(5), p.594-603, 1982.

Xiang, J. Evaluation of hydraulic conductivity of Carson County well field, Amarillo, Texas, Ground Water, 34(6), p. 1042-1049, 1996

Zhang, Z., and M. L. Brusseau. Characterizing three-dimensional hydraulic conductivity distributions using qualitative and quantitative geologic borehole data: Application to a field site, Ground Water, 36(4), p. 671 - 678, 1998.

US EPA ARCHIVE DOCUMENT

draft